Ecological Indicators 128 (2021) 107821

Contents lists available at ScienceDirect

Ecological Indicators

journal homepage: www.elsevier.com/locate/ecolind

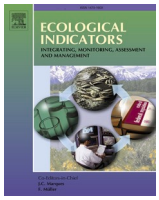

Original Articles

GIMMS NDVI3g+ (1982–2015) response to climate change and engineering activities along the Qinghai–Tibet Railway

Chao Ma [a,b,c], Tingting Li [a], Pei Liu [a,b,*]

[a] School of Surveying and Mapping Land Information Engineering, Henan Polytechnic University, Jiaozuo 454003, Henan, PR China
[b] Key Laboratory of Spatio-temporal Information and Ecological Restoration of Mines (Ministry of Natural Resources of the People's Republic of China, MNR), Henan Polytechnic University, Jiaozuo 454003, Henan, PR China
[c] Research Centre of Arable Land Protection and Urban-rural High-quality Development in Yellow River Basin, Henan Polytechnic University, Jiaozuo 454003, Henan, PR China

ARTICLE INFO

Keywords:
Qinghai–Tibet Railway
Xining to Golmud South–mountain Pass (XGSP)
Golmud South–mountain Pass to Lhasa (GSPL)
GIMMS NDVI3g+
Engineering activities
Climate change

ABSTRACT

Restricted by cold, drought and high altitude natural environments, vegetation ecological environment of the Qinghai–Tibet Plateau is fragile and difficult to repair when damaged. The purpose of this research is to reveal the characteristic of Normalized Difference Vegetation Index (NDVI) in direct impact area and ecological background area response to the engineering activities and global climate changes along Qinghai–Tibet railway. A framework was constructed by integrating a Gaussian fitting model, a buffer analysis, a trend analysis, a correlation analysis and a regression analysis method. The advantages of this framework are (1) Exploration of the impact of human and natural factors on the local vegetation ecological environment in *pre-*, *co-*, and *post-*construction of the railway; (2) Investigation of the time and extent of the impact of engineering activities on the plateau ecological environment; (3) Identify the contribution of climate change and engineering activities to changes of vegetation index. The framework was evaluated with GIMMS (Global Inventory Modeling and Mapping Studies) and MODIS (Moderate Resolution Imaging Spectroradiometer) NDVI from 1982 to 2001–2018. Results demonstrated that (1) Annual NDVI of the Qinghai–Tibet Railway was highly responsive to climate change and engineering activities, and shown a downward trend, upward trend for under construction and in operation period respectively. (2) Engineering activities of the Qinghai–Tibet Railway had a significant impact on vegetation along the route. Annual NDVI growth rate of 'core area' and 'background buffer' are quite different in pre-construction, under construction and in operation time. (3) Climate change along the Qinghai–Tibet Railway was significantly be responded to global changes during the 34 years. The air temperature and precipitation growth rate of the Golmud South–mountain Pass to Lhasa (GSPL) route is substantial lower than that of the Xining to Golmud South–mountain Pass (XGSP) route. Research results recommend that information on vegetation ecological environment is exploited by government agencies to ensure responsible ecological safety, traffic safety and sustainable development along the Qinghai–Tibet railway.

1. Introduction

The Qinghai–Tibet Plateau is a giant geomorphic unit with the low latitude, the high altitude, and the latest era in its formation period. Unique climatic conditions and geographical location lead to a sensitive and fragile ecosystem on the Tibetan Plateau (Niu et al., 2019). Restricted by various natural environments such as cold, drought, high altitude, etc., there are few species that can survive on the Qinghai–Tibet Plateau, and various types of animals and plants also have a short life cycle (Wang et al., 2015). This special entire ecosystem with low overall biomass, relatively simple formed biological chain, and the conversion rate of matter and energy is extremely slow. Therefore, if the ecological environment of the Qinghai–Tibet Plateau is damaged, it is very difficult to repair, and it may even cause serious environmental problems (Li et al., 2017).

The Qinghai–Tibet Railway, the South–to–North Water Diversion, West–to–East Gas Transmission, and West–East Power Transmission are called the four major projects of the Peoples' Republic of China, and the construction of Qinghai–Tibet Railway is of great significance to

* Corresponding author at: School of Surveying and Mapping Land Information Engineering, and Key Laboratory of Spatio-temporal Information and Ecological Restoration of Mines (Ministry of Natural Resources of the People's Republic of China, MNR), Henan Polytechnic University, Jiaozuo 454003, Henan, PR China
E-mail address: liupei@hpu.edu.cn (P. Liu).

https://doi.org/10.1016/j.ecolind.2021.107821
Received 6 August 2020; Received in revised form 27 March 2021; Accepted 21 May 2021
Available online 25 May 2021

Nomenclature

Symbol	Definition
r	is the value of Pearson's correlation coefficient, which represents the strength of the correlation between the two variables, and the value range is (−1, 1).
R	is the coefficient of determination.
R^2 (or R^2)	is the fitting degree of linear or nonlinear fit.
Sig.	is a abbreviation of the significant level.
P (*italic*)	is confidence level ($P < 0.05$ significant; $P < 0.01$ very significant)
n	is the number of samples.
P	is precipitation
T	is air temperature
τ	is the threshold value of the growing season

accelerate the economic and social development of the western region, especially for Tibet (Tibet Autonomous Region Railway Construction and Operation Leading Group Office Tibet Autonomous Region Development and Reform Commission, 2016). The engineering geological problems associated with large-scale projects have attracted wide attention, such as the engineering land generated during the construction of the Qinghai–Tibet Railway(Sun et al., 2010), soil removal operations (Luo et al., 2018a), construction access roads (Wang et al., 2009), inorganic matter and heavy metal pollution and other factors forming eco-disturbance corridors (Wu et al., 2016; Zhang et al., 2012a). As a result, changes in sunlight angle(Wu et al., 2011), water and heat conditions (Li et al., 2019; Zhang et al., 2019), surface runoff (Wang et al., 2019), and frozen soil structure (Wu et al., 2010) will block ecological water use (Chen et al., 2012) and destroy soil water holding capacity (Zhang et al., 2012b), further induce ecological and environmental problems.

Vegetation is the most important part of the ecosystem along the railway, and which has ecological functions such as regulating runoff, conserving water sources, maintaining biodiversity, soil and water conservation. Therefore, the quality of the local ecological environment is mainly determined by vegetation (Qin and Zheng, 2010). In recent years, many scholars have devoted to the study of the environmental impact along the Qinghai–Tibet Railway. Most studies originated in local alpine vegetation to explore the vegetation coverage, net primary productivity of vegetation, and changes in biomass along the railway. For instance, based on the field survey data from August 2001 and August 2002, Chen et al. (2003) realized that the implementation of the highway and railway project would directly cut the ecosystem along the route and make the landscape more fragmented, which would further result in the annual net primary productivity (NPP) of vegetation and biomass decreased. Ding et al. (2005, 2006) studied the changes in vegetation coverage along the Qinghai–Tibet Highway and Railway (1981–2001) before the construction of the Golmud–Lhasa section, and found that the changes in vegetation coverage in the study area tended to stabilize in the past 20 years. Zhang (2002) noticed that the Golmud–Lhasa section of the Qinghai–Tibet Railway used a huge amount of earth and stone. Moreover, the huge amount of earth and stone could cause a certain degree of damage to the surface vegetation, and further lead to land desertification, soil erosion, and wetland shrinkage. Zhang et al. (2002) studied the land use change and landscape pattern change in three counties (cities) along the Qinghai–Tibet Highway (Golmud–Tangula Mountain Pass), and found that the built-up in the study area increased rapidly, the cultivated-land decreased greatly, and the grassland was seriously degraded. Luo et al. (2018b) studied the impact of climate change and human activities on alpine vegetation and frozen soil in the Qinghai–Tibet Project Corridor (Golmud–Lhasa section) from 1981 to 2010, and discovered that climate warming and humidification could promote vegetation ecology, while project construction led to the degradation of alpine vegetation.

However, the above research was limited to ecological assessment of vegetation in certain sections (Golmud–Lhasa section for instance) and a certain period (early and middle period of the engineering activities), and it had not been able to compare the difference of the whole routine for a long term, as well as, to identify the respective contributions of climate change and engineering activities. In addition, when Xining–Golmud section and Golmud–Lhasa section have been in operation 15 and 35 years respectively, it will take the leading role in

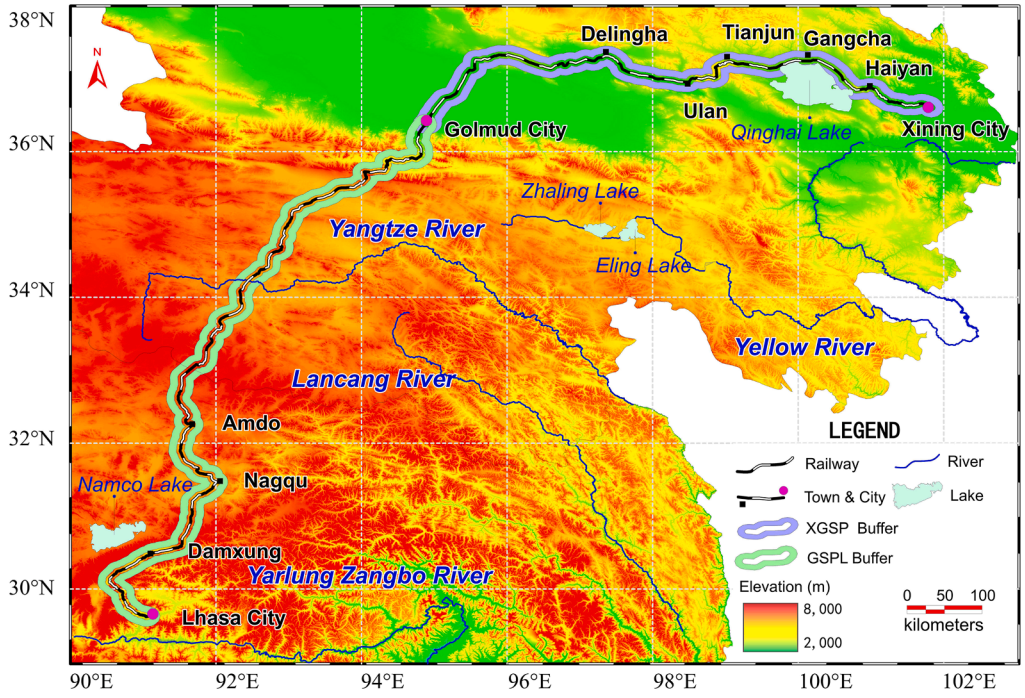

Fig. 1. Topography and Geography along the Qinghai–Tibet Railway.

ecological evolution and ecological restoration of major projects in ecologically fragile areas that continuing to pay sustainable attention to the characteristics of the ecological environment in the later stages of the railway. In this research, we intended to investigate the GIMMS NDVI3g + dataset changes in the long-term (1982–2015) temporal and spatial along the Qinghai–Tibet Railway, and explored the impact of human and natural factors on the local vegetation ecological environment before, during, and after the construction(or say *pre-*, *co-*, and *post-*construction) of the Qinghai–Tibet Railway. Furthermore, by studying the fluctuations of vegetation along the Qinghai–Tibet Railway, not only can explore and extent the impact of engineering activities on the plateau ecological environment as time went by, but also can indirectly provide data support for global warming issues, plateau grassland ecological restoration and ecological environment improvement.

2. Research area and dataset

2.1. Research area

Qinghai–Tibet Railway is from Xining, Qinghai Province in the east to Lhasa, Tibet Autonomous Region in the south, with a total length of 1 956 km (Fig. 1). Among them, the Xining to Golmud South–mountain Pass (XGSP)[1] is 814 km in length, built in 1979 and put into operation in 1984,. Golmud South–mountain Pass to Lhasa (GSPL)[2] is from Golmud, Qinghai Province in east to Lhasa, Tibet Autonomous Region in west, has a total length of 1 142 km, of which 1 107 km is a newly built road section, paved on October 12, 2005 (Chen et al., 2012). Eighty-five percentage of GSPL is located at an altitude of more than 4 000 m. The average annual temperature over GSPL is lower than 0 ℃. Furthermore, more than 550 km in this area is permafrost and the highest point is 5 072 m when across Tanggula Mountain. The Qinghai–Tibet Railway is the longest and highest altitude railroad built on the plateau on the world (Wu et al., 2016).

The Qinghai–Tibet Highway runs parallel to the Qinghai–Tibet Railway, with a design of the nearest distance of 2 km and the longest distance of 16 km. Considering its common impact and referring to literature review (Zhang, 2002; Zhang et al., 2002c), the direct impact area set in this study is an 8 km strip buffer zone including the Qinghai–Tibet Railway ("core area")[3], and the ecological background area is outside the Qinghai–Tibet Railway 8–16 km ring buffer ("background buffer")[4] (see Fig. 1)

2.2. Datasets

AVHRR (advanced very high resolution radiometer) NDVI (normalized difference vegetation index) is global continuous dataset with the longest coverage time by far, especially the GIMMS (global inventory modeling and mapping studies) NDVI dataset, which has undergone three generations of updates and has advantages of long time series, wide coverage, and the ability to characterize the dynamic changes of vegetation (Dardel et al., 2014; Tucker et al., 2005, 2001). AVHRR GIMMS NDVI has become one of the most widely used datasets, and has been widely used in the field of vegetation change monitoring and vegetation productivity simulation at the regional and/or global scale (Piao and Fang, 2002; Zhang et al., 2013a).

GIMMS NDVI3g + is an enhanced third-generation long-term GIMMS AVHRR NDVI data set (https://ecocast.arc.nasa.gov/data/pub/) of VI3g (1981.7–2013.12) published by the National Aeronautics and Space Administration (NASA). The data set adopts the WGS84 world geodetic coordinate system, equal latitude/longitude projection, with a 15d temporal resolution and a 0.0833° (1/12°×1/12°) spatial resolution. Selected dataset can obtained from NOAA/AVHRR series of satellites (NOAA7, NOAA9, NOAA11, NOAA14, NOAA16, NOAA17, NOAA18, NOAA19), the data set has been officially performed atmospheric correction, geometric rough correction, geometric fine correction, delete bad lines and eliminate the impact of volcanic eruptions, in addition to considering global factors, the data set has also been processed for short-term effects of atmospheric aerosols and cloud cover to ensure the quality (Ana et al., 2017). So in global vegetation research community, the dataset is considered to be the most valuable data source, and has a unique advantage in large-scale vegetation research (Goetz et al., 2006; Kobayashi and Dye, 2005).

The selected meteorological data comes from the annual climate dataset (1982–2015) provided by the Resource and Environmental Data Cloud Platform (http://www.resdc.cn), and performed Kriging interpolation in ArcGIS© to obtain the national annual average temperature and annual average precipitation climate data, which have a same spatial resolution as the GIMMS data. The 34a average temperature and average precipitation information of Qinghai–Tibet Railway core area and buffer zone images were obtained by vector data cropping in batches. It also includes a 1:1 million Chinese vegetation map.

3. Methodology

GIMMS NDVI3g + is the semi-monthly synthetic data generated by the Maximum Value Compositing method (MVC)[5]. In this study, we furthered to composite monthly NDVI data and annual NDVI data using the same approach. At the same time, the vector data of "core area" and "background buffer" of the Qinghai–Tibet Railway were selected to obtain the average temperature and average precipitation information along Qinghai–Tibet Railway by batch-cutting the 34a climate annual data set (1982–2015). Based on average temperature and average precipitation information, the inter/inner annual NDVI and climate analysis fundamental dataset were generated.

3.1. Gaussian fitting

Gaussian function is a probability density function representing continuous random variables. It is usually used to express the periodic evolution of natural phenology (Li and Sheng, 2008). The one-dimensional expression of the function (unimodal) is as follows:

$$y = y_0 + \frac{A}{w \cdot \sqrt{\pi/2}} e^{-\frac{2(x-x_0)^2}{w^2}} \quad (1)$$

Where, y_0 is offset of the baseline. A is the integral area under the bell curve (NDVI equivalent biomass). x_0 is the height of the center peak (equivalent mathematical expectation). $w = 2\sigma$ is approximately equal to 0.849-time width at half of the peak height (when the peak height is 1/2, the width of the bell curve), this value represents the length of the growing period when the vegetation is flourish.

3.2. Trend analysis

The univariate linear regression analysis method can simulate the change trend of each grid and reflect the spatial characteristics of NDVI change trend in different periods. Fitting with data of all years to avoid the randomness and incidental of research results, and outcomes can more accurately reflect the growth status and changing trends of vegetation (Hou et al., 2013; Lv et al., 2014). The formula can be expressed as:

[1] The Xining to Golmud South-mountain Pass, XGSP.
[2] The Golmud South-mountain Pass to Lhasa, GSPL.
[3] The direct impact area set in this study is an 8 km strip buffer zone including the Qinghai−Tibet Railway.
[4] The ecological background area is outside the Qinghai-Tibet Railway 8–16 km ring buffer.
[5] The Maximum Value Compositing, MVC

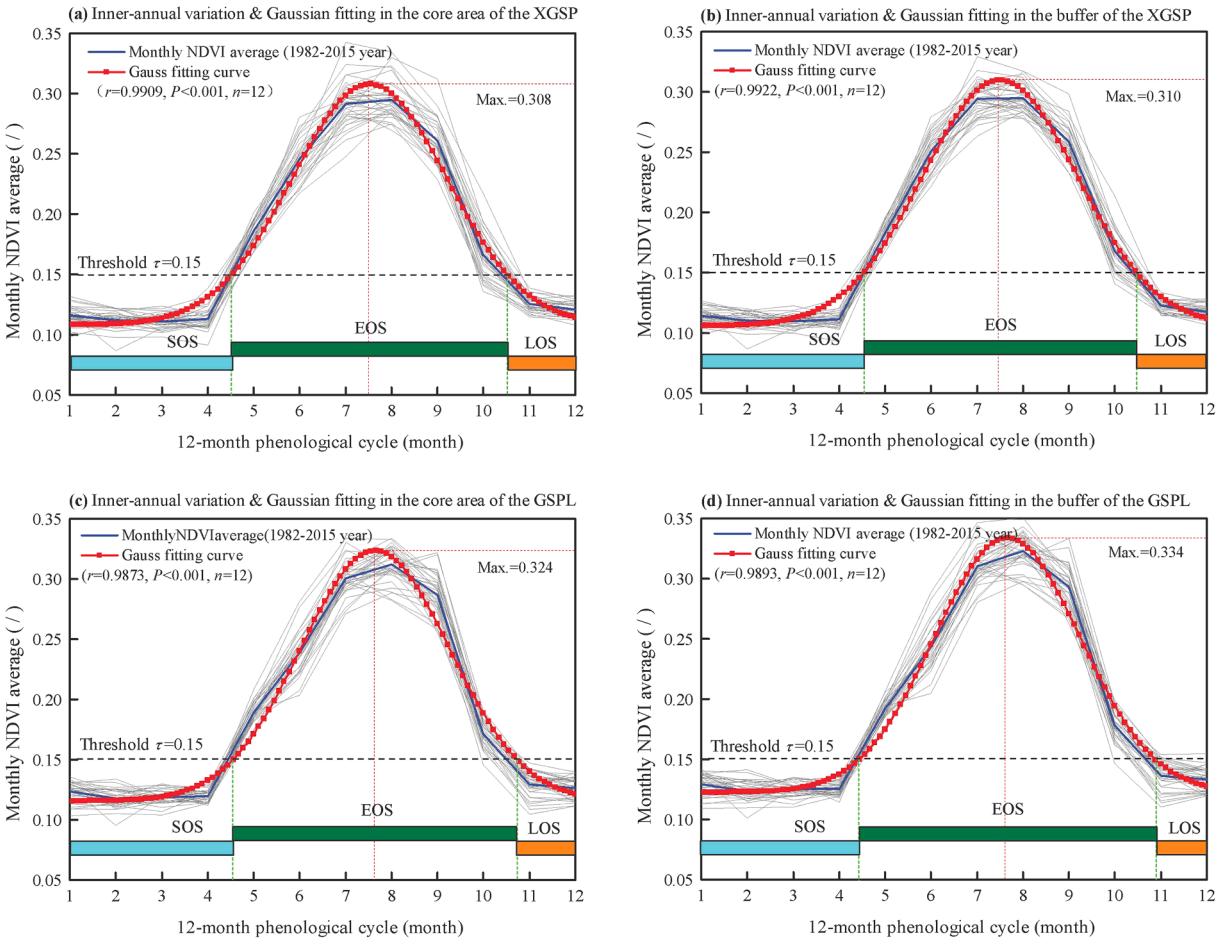

Fig. 2. Inner-annual variation and Gaussian fitting of NDVI on Qinghai–Tibet Railway (r is the Pearson's correlation coefficient among monthly NDVI and the GAUSS fitting values.)

$$\theta_{slope} = \frac{n \times \sum_{i=1}^{n}(i \times NDVI_i) - \left(\sum_{i=1}^{n} i\right)\left(\sum_{i=1}^{n} NDVI_i\right)}{n \times \sum_{i=1}^{n} i^2 - \left(\sum_{i=1}^{n} i\right)^2} \quad (2)$$

Where, θ_{slope} is the slope of the NDVI regression equation in pixel (i.e., coefficient of regression), n is the number of monitoring years, $NDVI_i$ is the NDVI value of the ith year. When$\theta_{slope} > 0$, it means the vegetation index of the pixel increases with time, and vegetation coverage shows an increasing trend; otherwise, the vegetation index shows a downward trend.

3.3. Correlation analysis

Correlation analysis is used to study the interaction between two specific variables (Liu et al., 2013). The formula for calculating correlation coefficient is:

$$r_{xy} = \frac{\sum_{i=1}^{n}(x_i - \bar{x})(y_i - \bar{y})}{\sqrt{\sum_{i=1}^{n}(x_i - \bar{x})^2 \sum_{i=1}^{n}(y_i - \bar{y})^2}} \quad (3)$$

Where, r_{xy} is the correlation coefficient of variables x and y, i is the number of samples; x_i is the MNDVI of ith year, y_i is annual average temperature or precipitation; $\bar{x}$ is the ANDVI from 1982 to 2015; $\bar{y}$ is cumulative average temperature or average precipitation for the corresponding period.

3.4. Coefficient of variation

The coefficient of variation indicates the degree of relative change (fluctuation) of geographic data (Lei et al., 2019). Hence, the coefficient of variation was selected to analyze the stability of vegetation changes. The calculation formula is:

$$Cv = \frac{1}{\bar{x}}\sqrt{\frac{\sum_{i=1}^{n}(x_i - \bar{x})^2}{n-1}} \quad (4)$$

Where, Cv represents the coefficient of variation of the MNDVI, n is the number of monitoring years, x_i is NDVI of ith year, $\bar{x}$ is the ANDVI from 1982 to 2015; the larger the Cv value is, the greater the NDVI fluctuation is; the smaller the Cv value is, the smaller the NDVI fluctuation is.

4. Results

4.1. Change results of inner-annual

The Qinghai–Tibet Railway is a long and narrow ecological corridor. Area of Qinghai–Tibet Railway spans 9 geographic latitudes (29°~38°N) and 12 geographic longitudes (90°~102°E), the height difference of this area is 4 300 m (altitude from 2 200 m to 6 500 m), the surface cover is extremely uneven. So on the basis of MVC monthly compositing NDVI data, the monthly average of NDVI3g + was calculated through that NDVI value of the entire area was accumulated and divided by the number of pixels (also called the average value compositing method:

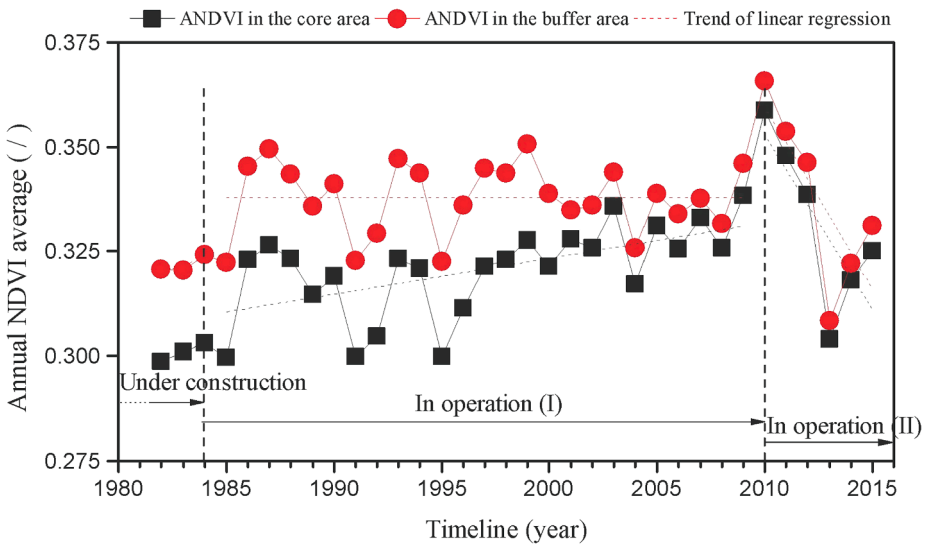

Fig. 3. Piecewise linear regression analysis of the inter annual variation of the ANDVI in the XGSP.

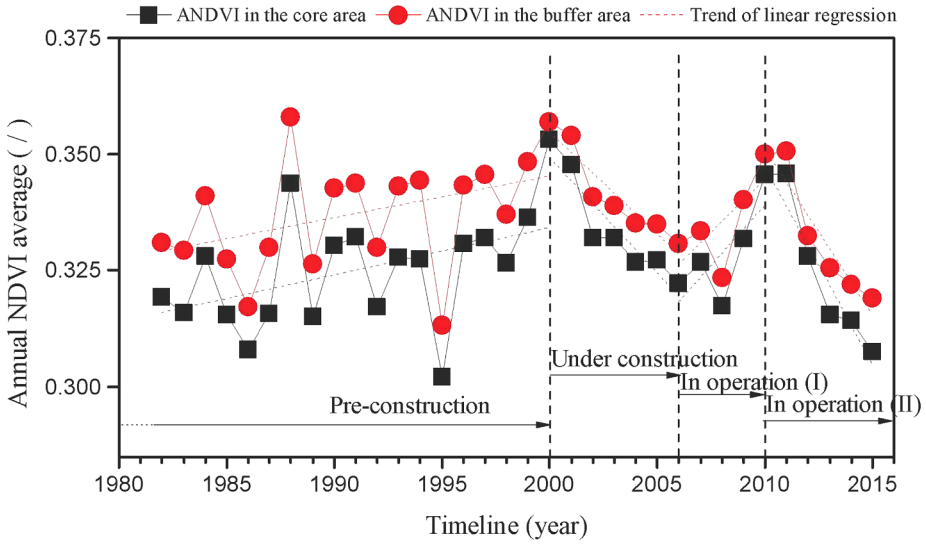

Fig. 4. Piecewise linear regression analysis of the inter-annual variation of the ANDVI in the GSPL.

here, ANDVI=∑NDVI/n). In this way, the two railway sections (XGSP, GSPL) had a total of four areas (two "core area", two "background buffer"), and 408 monthly average datasets were obtained in 34a.

Shown as Fig. 2, no matter "core area" or "background buffer", the strongest vegetation growth period along the Qinghai–Tibet Railway in a year occurred between July and August and the NDVI showed a single-peak change trend, which was consistent with the Gaussian distribution and consistent with the annual growth cycle of plants in the area (Yan et al., 2005).

In response to this feature, we quoted the GAUSS function (Eq.(1)) to fit the 34a average NDVI (see also Fig. 2, $P < 0.001$), and then used the threshold method to determine the start of the season (SOS)[6], the end of the season (EOS)[7], timing of maximum of the growing season by peak vegetation indices, and the length of growing season (LOS)[8] or duration of greenness. By literature review (Luo et al., 2018b; Zhang et al., 2013b), the threshold value ($\tau = 0.15$) was substituted into the Gaussian fitting Eq. (1), and calculated SOS (x_1), EOS (x_2) and LOS (x_2–x_1). The average growth period of vegetation in the XGSP is 182 days, and the average growth period of vegetation in the GSPL is 190 days (see S1). This is closely related to the physical and geographical conditions of the two road sections.

4.2. Change results of inter-annual

The 34a inter-annual time series change curves were be obtained by sum of annual average NDVI (ANDVI) divided by the number of pixels.

The XGSP planned to build in 1950, built in 1979 and put into operation in 1984. The 34a time series NDVI could be roughly divided into three stages, namely the construction period before 1984 and the operation stage (I) during 1985 to 2009, and the operation stage (II) after 2010. Research results demonstrated that the ANDVI of the "background buffer" is better than that of the "core area", and the gap between the two regions is large during the construction period. There was a significant improvement in the initial stage of operation, and the

[6] The start of the vegetation-growing season, SOS.

[7] Onset of senescence or time of end of greenness as the end of the season, EOS.

[8] Timing of maximum of the growing season by peak vegetation indices, and the length of growing season or duration of greenness, LOS.

Table 1
Piecewise linear regression equation of the ANDVI annual variation in Qinghai–Tibet Railway.

	Inter-year	Before construction	Construction	Operation	Operation (2010–2015)
XGSP	"core area"	No data	$\hat{y}$=0.00216x−3.982(r = 0.999, Sig. = 0.026*)	$\hat{y}$=0.00108x−1.840(r = 0.588, Sig. = 0.002**)	$\hat{y}$=−0.00834x + 17.117(r = −0.774, Sig. = 0.071)
	"background buffer"	No data	$\hat{y}$=0.00171x−3.069(r = 0.827, Sig. = 0.328)	$\hat{y}$=0.00024x−0.148(r = 0.005, Sig. = 0.980)	$\hat{y}$=−0.00872x + 17.893(r = −0.768, Sig. = 0.074)
GSPL	"core area"	$\hat{y}$=0.00101x−1.694(r = 0.464, Sig. = 0.045*)	$\hat{y}$=−0.00495x + 10.257(r = −0.931, Sig. = 0.002**)	$\hat{y}$=0.00518x−10.082(r = 0.757, Sig. = 0.138)	$\hat{y}$=−0.00902x + 18.471(r = −0.961, Sig. = 0.002**)
	"background buffer"	$\hat{y}$=0.00089x−1.446(r = 0.418, Sig. = 0.075)	$\hat{y}$=−0.00436x + 9.084(r = −0.944, Sig. = 0.001**)	$\hat{y}$=0.00455x−8.804(r = 0.715, Sig. = 0.174)	$\hat{y}$=−0.00734x + 15.107(r = −0.949, Sig. = 0.004**)

Note: * indicates that the regression equation did pass the significance test of $P < 0.05$; ** indicates that the regression equation did pass the significance test of $P < 0.01$.

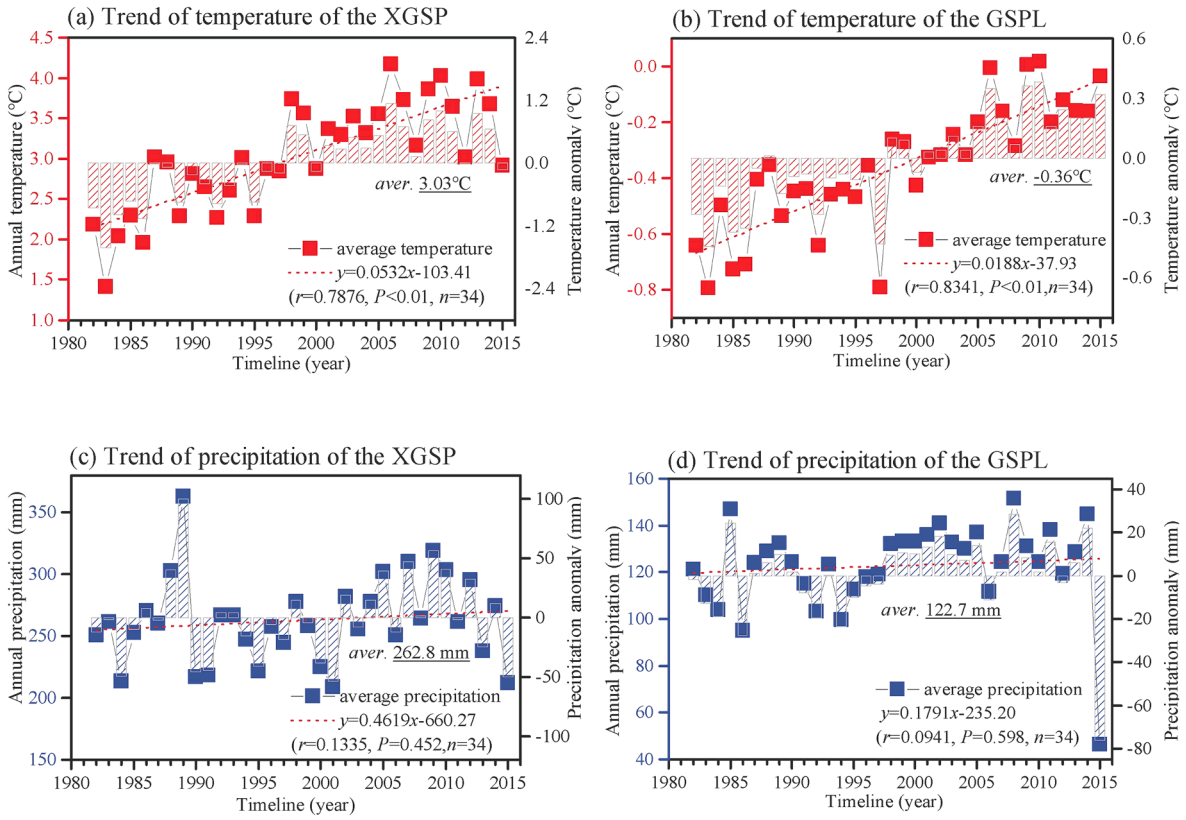

Fig. 5. The trend of average temperature & precipitation in the XGSP and the GSPL.

gap gradually narrowed thereafter (see Fig. 3).

The construction of GSPL started on June 29, 2001, and opened to traffic on July 1, 2006. Therefore, the NDVI of this section can be divided into four stages according to the time series, before construction (1982–2000), construction stage (2001–2005), in operation stage (I) (2006–2009), and in operation stage (II) (2010–2015). By analysis, the ANDVI of the "background buffer" is better than that of the "core area", the gap during the construction period is large, and the gap during the operation period is gradually narrowing shown as Fig. 4.

Due to the influence of engineering staged construction and operation, it needed to be analyzed ANDVI changes in stages. The piecewise linear fitting was used to obtain characteristics of the annual change of the Qinghai–Tibet Railway (see Table 1)

It can be seen from Table 1 that, in the XGSP, the ANDVI growth rate (i.e., the slope of the linear regression equation θ_{slope}, see also Eq. (2)) in the "core area" is 0.022/10a higher than that of "background buffer" is 0.017/10a for the construction period (1982–1984); ANDVI growth rate is 0.011/10a and 0.002/10a for "core area" and "background buffer" respectively in operation period (1985–2015). The ANDVI growth rate of "core area" was significantly greater than that of "background buffer" Results from Table 1 also indicated that, in the GSPL, change rate of NDVI was highly responsive to the railway construction process. Before the construction of the Qinghai–Tibet Railway (1982–2000), the ANDVI showed an overall upward trend for both "core area" and "background buffer" along the railway line. Growth rate of the ANDVI in "core area" was 0.010/10a and that in "background buffer" is 0.009/10a. While, during the construction period (2001–2006), growth rate of the ANDVI shown a downward trend, where the rate of average NDVI decline is –0.049/10a for the "core area" and is –0.044/10a for the "background buffer". The ANDVI had a large fluctuation during the operation period (2007–2015), in the early stage of operation (2007–2010) the ANDVI had an overall increasing trend, in which the growth rate of the "core area" is 0.052/10a, the growth rate of "background buffer" is 0.046/10a; in the later period of operation (2011–2015), the ANDVI shown a downward trend.

From 2010 to 2015, ANDVI of all Qinghai–Tibet Railway shown a downward trend. Liu, et al. (2013) indicated that since 2010, precipitation has continued to decline, and the global climate change leading to

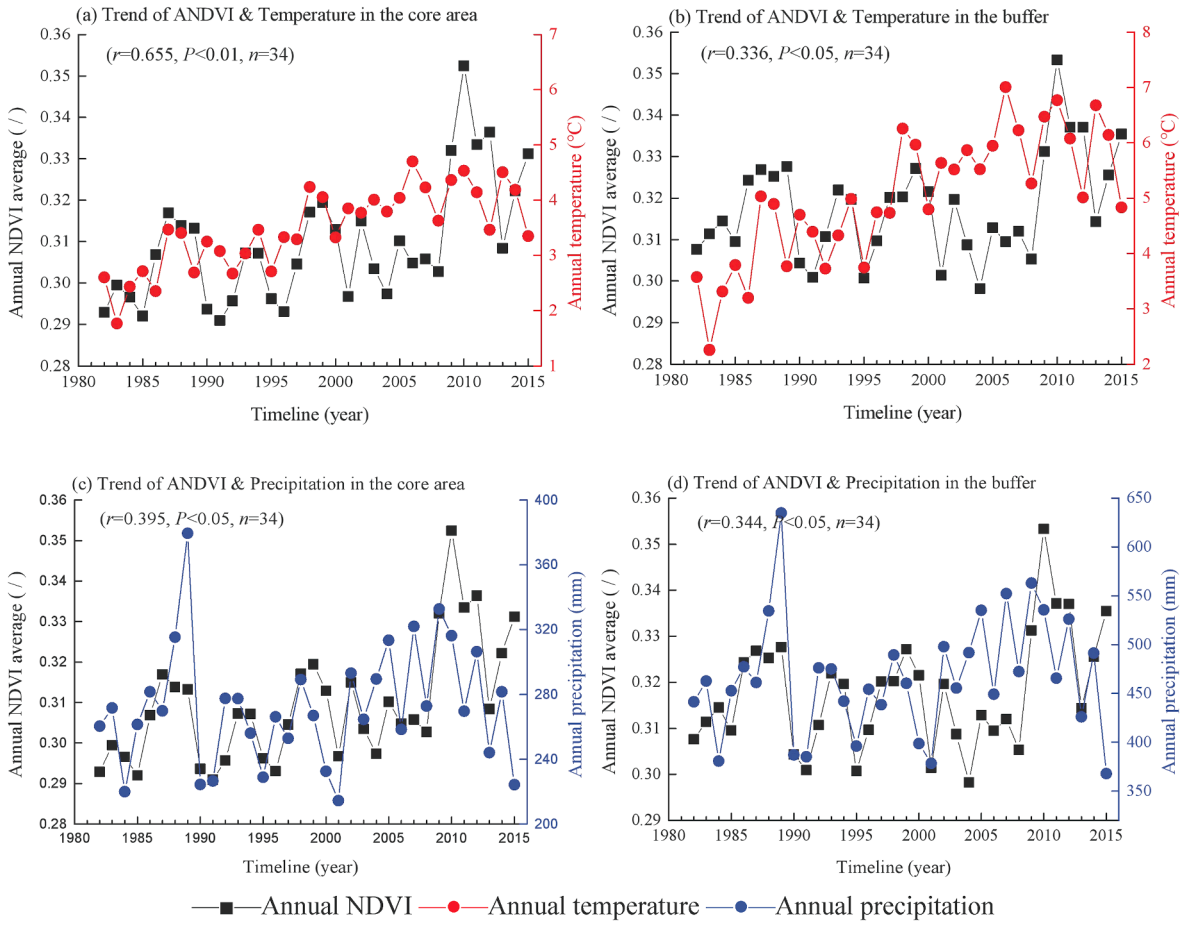

Fig. 6. Correlation between the ANDVI and climatic factors in XGSP.

the decline of vegetation.

4.3. *Climate change and response to NDVI*

1) Climate change

Since the distance between "core area" and "background buffer" is only 8 km, the method of (combining the two areas) global average was used to calculate the average temperature and precipitation. The time series average temperature of the XGSP and the GSPL is shown as the Fig. 5a and 5b, the time series average precipitation of the XGSP and the GSPL is shown as the Fig. 5c and 5d. Characteristics of temperature and precipitation over the study area can be found in S2.

Fig. 5 demonstrated that ① In the past 34 years, temperature along the Qinghai–Tibet Railway has increased. For XGSP, the average temperature is 3.5 ℃ with a growth rate of 0.57 ℃/10a in "core area"; the average temperature is 3.6 ℃ with a growth rate of 0.50 ℃/10a in "background buffer" (Fig. 5a). While for GSPL section, the average temperature is –0.31 ℃ with a growth rate of 0.20 ℃/10a in "core area"; the average temperature is –0.41 ℃ with a growth rate of 0.18 ℃/10a in "background buffer" (Fig. 5b).

② In the past 34 years, precipitation along the Qinghai–Tibet Railway has been increasing slowly. For XGSP, the average precipitation is 272.4 mm with a growth rate of 4.67 mm/10a in the "core area"; the average precipitation in "background buffer" is 253.2 mm with a growth rate of 4.57 mm/10a. The results are not significant due to the large fluctuations in precipitation. According to literature review, heavy rainfall events occurred allover China in 1989, and an abnormally heavy rainfall of 379.4 mm in the XGSP, catastrophic flood out broken in the Golmud River, and Chaerhan Salt Lake area (Lei et al., 2019; Liu et al., 2013) (Fig. 5c). And for GSPL, the average precipitation is 127.7 mm with a growth rate of 1.79 mm/10a in the "core area", while an abnormally low value of 48.1 mm occurred in 2015; the average precipitation was 117.8 mm with a growth rate of 1.78 mm/10a in "background buffer", and the abnormally value in 2015 was 44.6 mm (Fig. 5d).

2) NDVI response to Climate change

We combined time series of the annual average NDVI (ANDVI) with the annual average temperature and annual average precipitation to obtain the ANDVI change trend and the coupling relationship. According to Eq. (3), the correlation coefficients between the ANDVI and the annual average temperature, annual precipitation from 1982 to 2015 can be calculated to determine the degree of response of the "core area" and the "background buffer" to climate change (see Figs. 6 and 7).

Fig. 6 shown that the ANDVI of the XGSP located in the arid and cold region is in good consistency with change trends of annual average temperature and precipitation, and the whole sections are significantly correlated (see S3). It is also demonstrated that the XGSP located in Qaidam Basin, in the past 34 years, the increasing of temperature and precipitation are beneficial to the growth of vegetation, which is consistent with the research conclusions of Lihui Luo et al. (Luo et al., 2018b).

The changes of the ANDVI and climate of GSPL are shown in Fig. 7. In general, only the "core area" of GSPL is significantly correlated with annual average precipitation r = 0.366 ($P < 0.05$, $n = 34$), while it is uncorrelated in "background buffer" (see S3). However, further research indicated that the correlation between the ANDVI and the annual average temperature in the GSPL has changed significantly around 2000. From 1982 to 1999, the ANDVI and temperature was significantly correlation; but from 2000 to 2015, the ANDVI and the temperature was not uncorrelated.

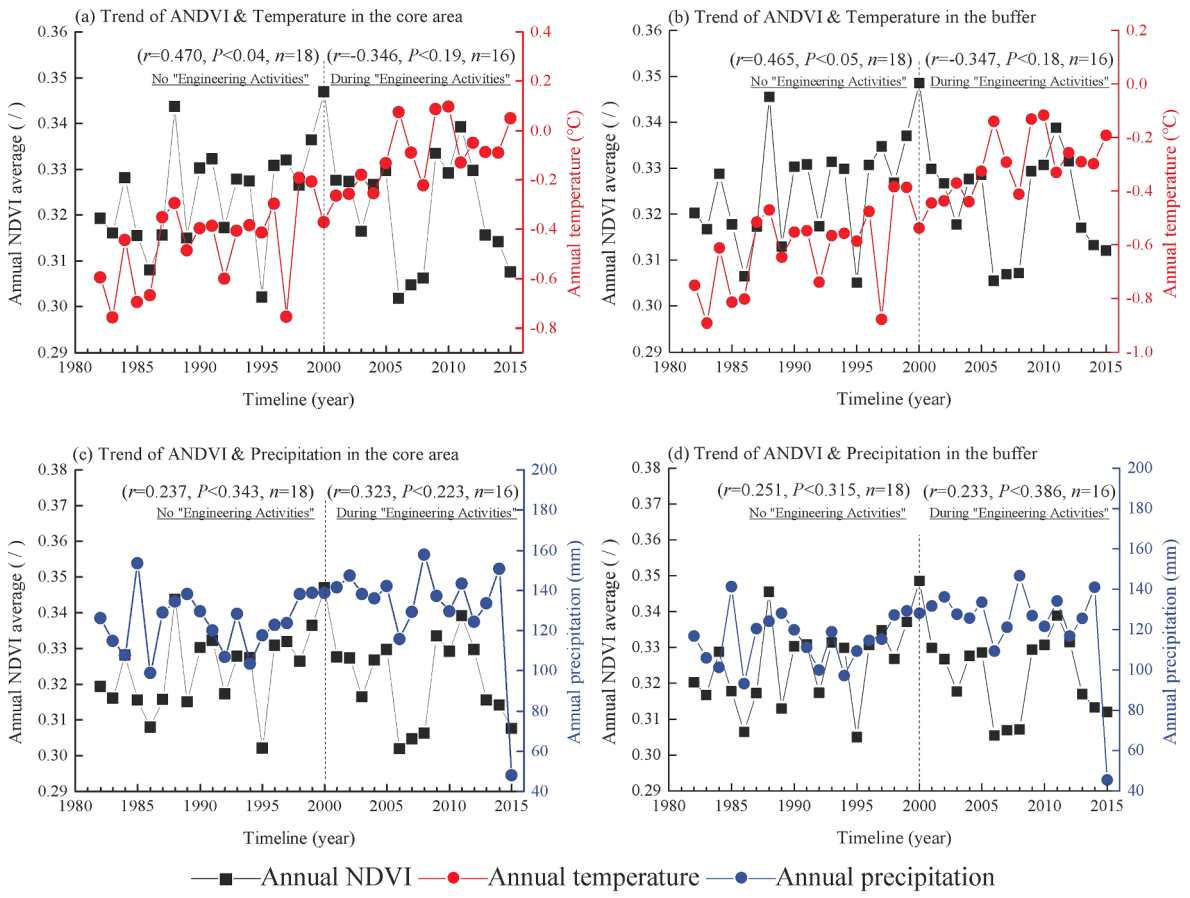

Fig. 7. Correlation between the ANDVI and climatic factors in GSPL.

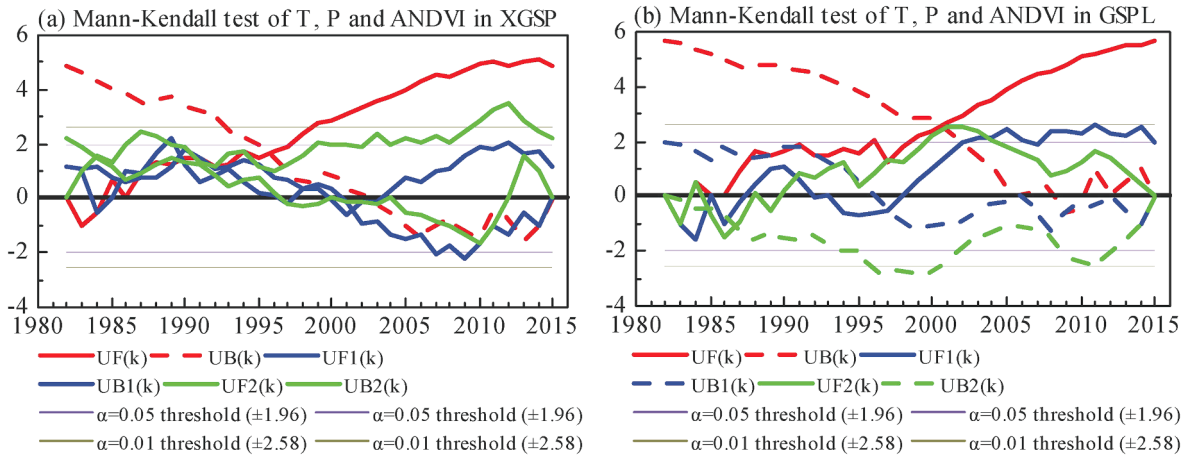

Fig. 8. The M−K test of T, P and ANDVI in the Qinghai–Tibet Railway. Note: The order statistic curve $UF_i(k)$and the reverse order statistic curve $UB_i(k)$represent annual average temperature (red), annual average precipitation (blue), and annual average NDVI (green), respectively. (For interpretation of the references to colour in this figure legend, the reader is referred to the web version of this article.)

3) Nonparametric mutation test

Diagnosing the impact of extreme climate and hydrological events on NDVI is a prerequisite for effectively separating the impact of climate change and engineering activities on environmental and ecological processes. Here, the Mann-Kendall test method (M−K test) among many change points diagnosis methods of catastrophe theory is introduced. M−K test is a non-parametric test method which widely applied to trend test of time series data. This method, follows neither some distribution characteristics nor disturbed by a handful of abnormal values, is suitable for abnormal distribution such as hydrological, ecological and meteorological data (Güçlü, 2020). The M−K mutation test results of the time series annual NDVI (ANDVI), temperature (T) and precipitation (P) were shown in Fig. 8.

From Fig. 8, it can be seen that in the XGSP section, annual temperature (red) had a sudden change (i.e., the intersection of the order statistical UF curve and the reverse order statistical UB curve.) in 1996, in which passed the hypothesis test with a $\alpha = 0.01$ confidence level. Annual precipitation (blue) fluctuated violently, with sudden changes in

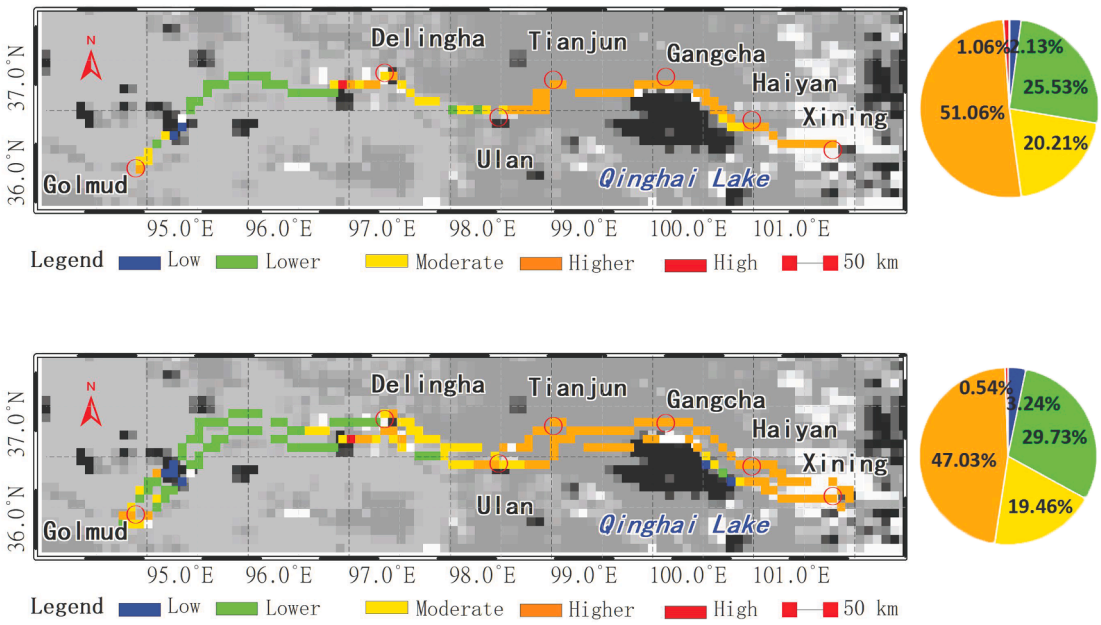

Fig. 9. GIMMS NDVI coefficient of variation in XGSP during 34-year.

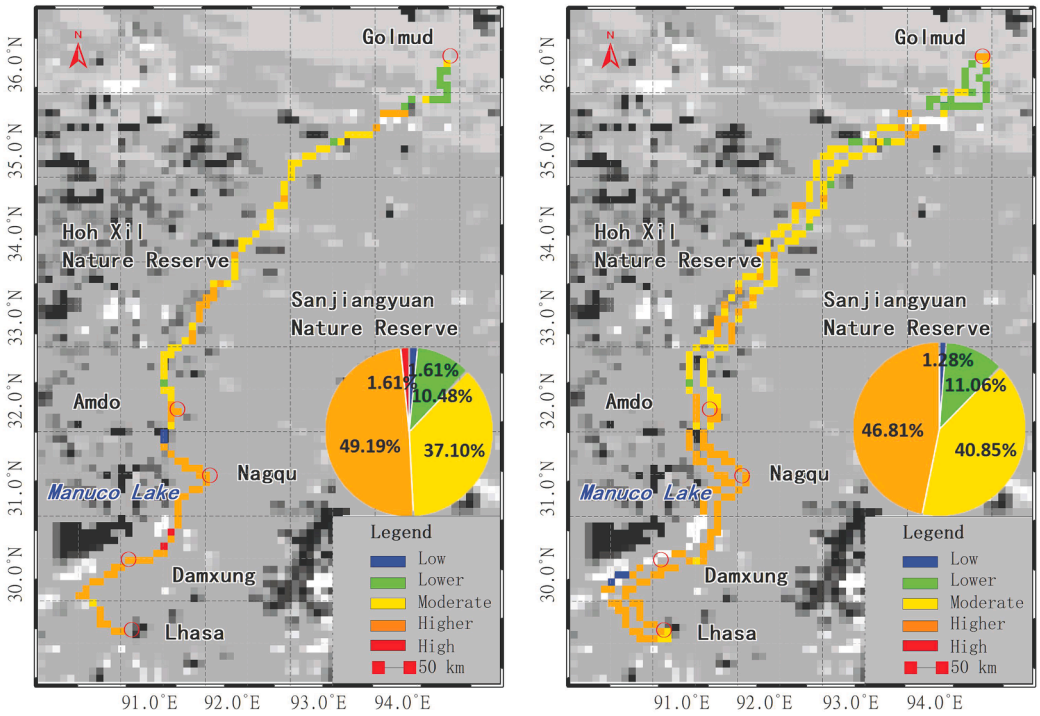

Fig. 10. GIMMS NDVI coefficient of variation in GSPL during 34-year.

1986, 1990 and 2001 respectively, but none of them passed the $\alpha = 0.05$ confidence level. ANDVI (green) only had a mutation point in 1984, in which passed the $\alpha = 0.05$ confidence level (see Fig. 8a). By analogy, in the GSPL section, annual temperature (red) had a mutation point in 2001, in which passed the hypothesis test with a $\alpha = 0.01$ confidence level. Annual precipitation (blue) had a mutation point in 1997, in which passed the $\alpha = 0.05$ confidence level. ANDVI (green) had mutations in 1985, 1987 and 2015, respectively, in which all of them passed the hypothesis test with a $\alpha = 0.01$ confidence level (Shown as Fig. 8b).

The M−K test shown that in the XGSP section, ANDVI had an abrupt event in 1984, which coupled with the engineering activities of railway construction, but had no coupling relationship with climate change. In the GSPL section, ANDVI has multiple mutation points, but there was no engineering activity coupled with railway construction.

4.4. Variation coefficient of GIMMS NDVI

The NDVI variation coefficient C_v of "core area" and "background buffer" in XGSP, GSPL between 1982 and 2015 can be calculated pixel by pixel according to Eq. (4). The NDVI variation coefficients C_v of "core area" and "background buffer" of the two sections are shown in Figs. 9 and 10 (the background is 1:1 million gray scale Chinese vegetation

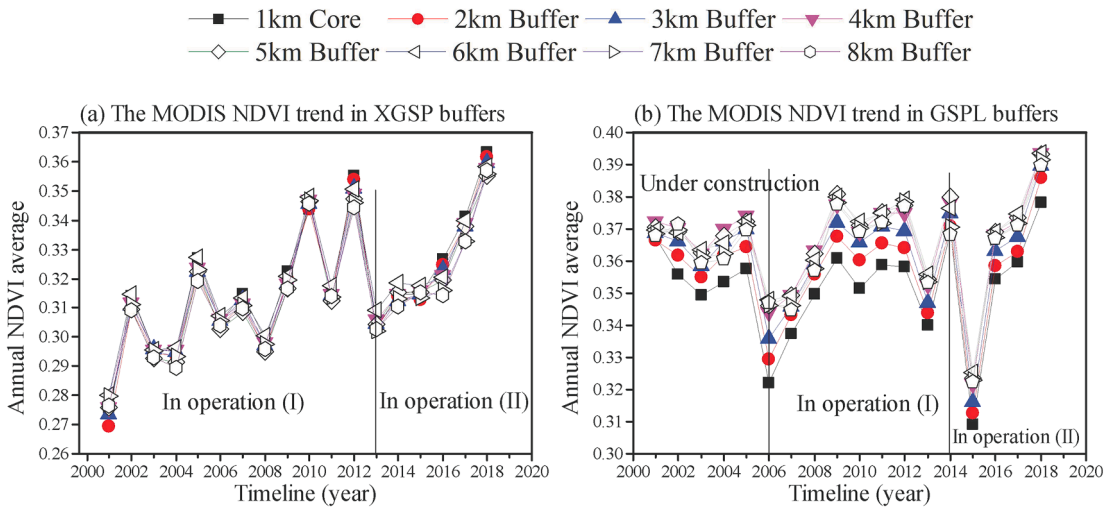

Fig. 11. Analysis of the MODIS ANDVI changes using multiple buffers.

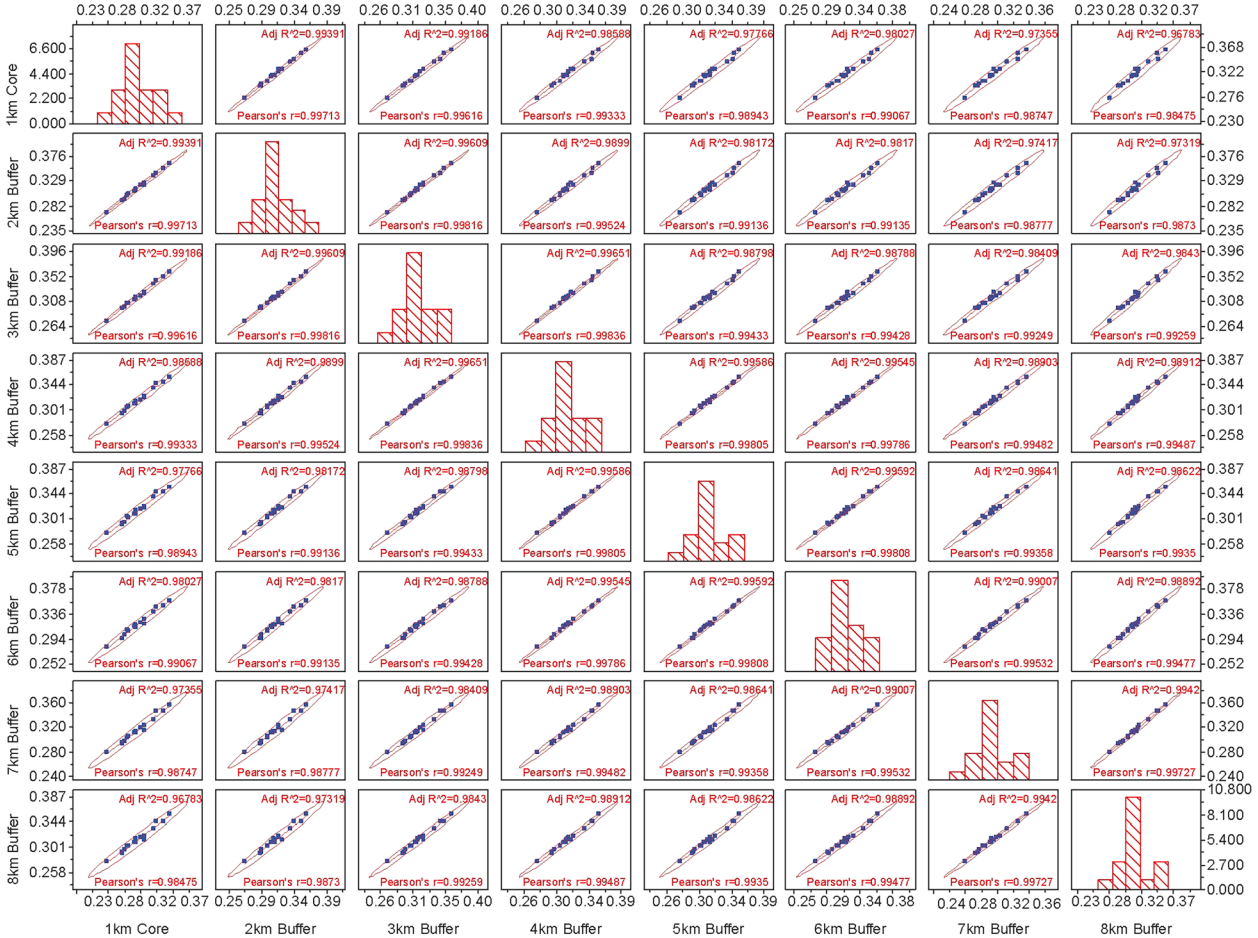

Fig. 12. Scatter matrix of multi-buffers ANDVI in XGSP (*r* is the Pearson correlation coefficient, R^2 is the fitting degree of linear fit, and the confidence level of the confidence ellipse is set to 97%.)

coverage map: Globeland cover30, GLC30[9]).

The C_v is divided into 5 levels (Ana et al., 2017): low, lower, moderate, higher and high. The XGSP is dominated by higher fluctuations (mainly distributed along Qinghai Lake) is about 50%, and lower fluctuations (mainly distributed along Qaidam Basin from Delingha to Golmud) is about 30%; the GSPL is dominated by higher fluctuations (mainly distributed alone Amdo-Lhasa segment) and moderate fluctuations (mainly distributed in the Hoh Xil permafrost area) is about 80%. The volatility of "core area" is slightly higher than "background buffer" (see S4).

[9] GlobeLand30 refers to the land cover of the earth between latitude 80N to 80S. http://www.globallandcover.com/GLC30Download/index.aspx

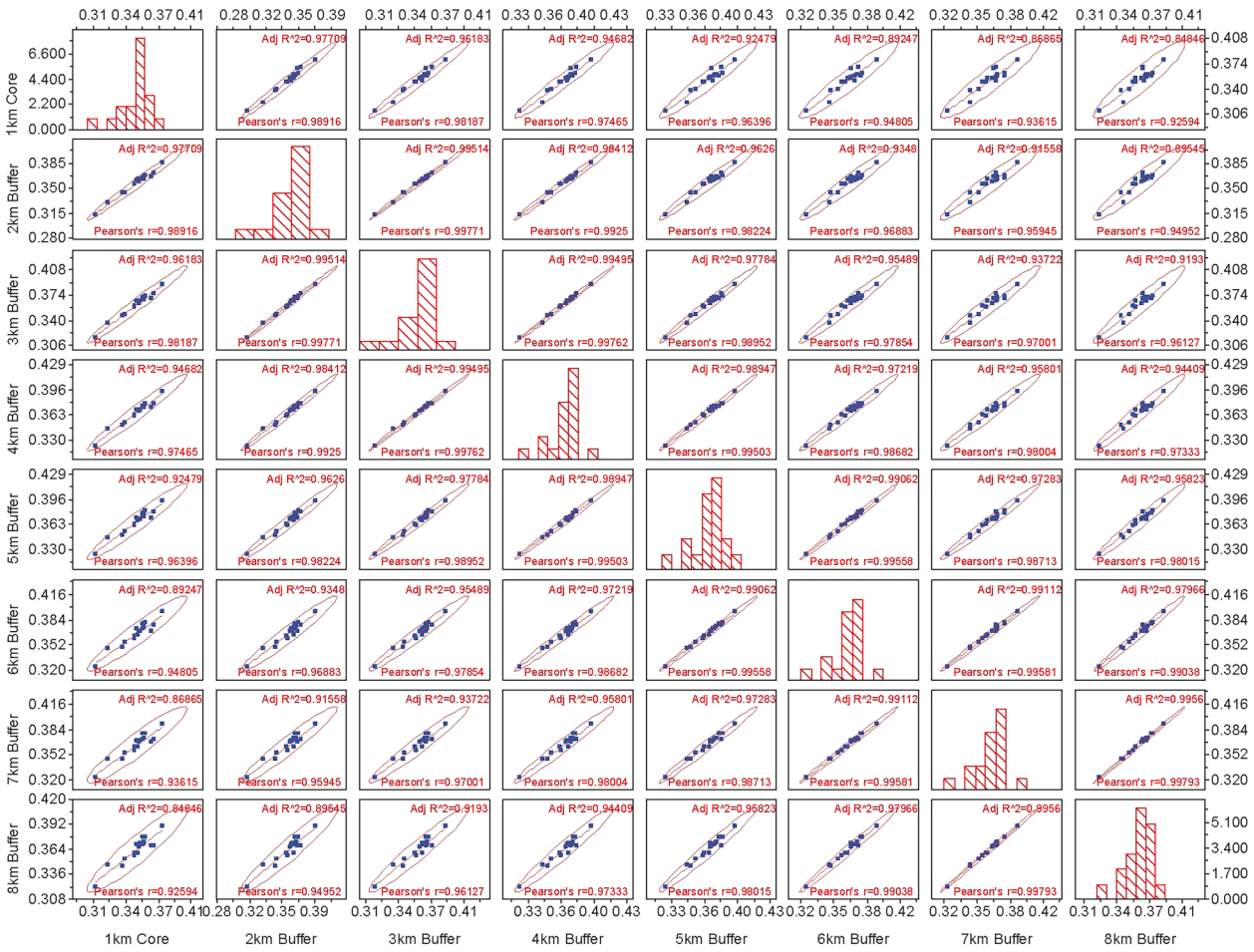

Fig. 13. Scatter matrix of multi-buffers ANDVI in GSPL (*r* is the Pearson correlation coefficient, R^2 is the fitting degree of linear fit, and the confidence level of the confidence ellipse is set to 97%.)

5. Discussion

5.1. Ecological sensitivity test and evaluation

In order to obtain the foundation of "background buffer" setting, in this research, vegetation index MOD13A2 of MODIS NDVI products (2001–2018) were selected to carry out the buffer ecological sensitivity test, and MODIS NDVI was used to verify the data overlap period (2001–2015) of GIMMS NDVI.

1) Ecological sensitivity test in buffers

A 1 km-wide core area is set along the Qinghai–Tibet Railway Using the MODIS NDVI (2001–2018) MOD13A2 vegetation index product. Based on the 1 km core area, buffers of 1–2 km, 2–3 km, 3–4 km, 4–5 km 5–6 km, 6–7 km, and 7–8 km, were setting with a width of 1 km, and the annual average MODIS NDVI (ANDVI) was calculated for each buffer (Fig. 11).

It can be seen from Fig. 11(a) that the ANDVI of all buffers had little difference, and approximately shown as two stages change of the XGSP which have been built for many years. The ANDVI fluctuations increased from 2001 to 2013, and continued to rise from 2013 to 2018. While, Fig. 11(b) demonstrated that the difference of the ANDVI of buffers are relative large and with three-stage changes in general of the GSPL. The ANDVI shown a downward trend from 2001 to 2006, fluctuations increased from 2006 to 2014, and continued rising from 2014 to 2018.

The following is a further statistical test we have done. The scatter matrix represents the correlation between multi-series ANDVIs in different buffers. When buffer zone is larger than 5 km, the correlation has a steep drop (especially in GSPL line). On the basis of this analysis, 8 km (4 km on both side) is set as direct influence zone.

Shown as Fig. 12, the 8 buffer zones used for sensitivity experiments have high correlation with each other, indicating that good ecological restoration and relatively stable vegetation coverage around XGSP of the Qinghai–Tibet Railway, which has been in operation for many years, although Pearson correlation still captures a small transition, changed from 0.997**, 0.996**, 0.993** to 0.989** for buffer zone from 1 km to 4 km.

Shown as Fig. 13, correlation between the 8 buffer zones used for ecological sensitivity experiments in GSPL has changed greatly, which demonstrate that the vegetation coverage around the GSPL of the Qinghai–Tibet Railway has changed greatly during the construction period. As the buffer zone expands with 1 km, Pearson correlation coefficients changed as 0.989**, 0.982**, 0.975**, 0.963** et al. Therefore, we set the significance level to 0.0005 instead of 0.001 as the sensitive mutation threshold.

In general, the ANDVI in the core area is less than that of all buffers. The ANDVI of the buffers continued to increase from the inside to the outside, which fully demonstrates the construction and operation of Qinghai–Tibet Railway caused diversity in the surrounding vegetation. The spatial and temporal correlation are obvious, the 4th outer level buffer still shown a differentiation from the inner layer (the 3rd level buffer zone), but the difference is significantly reduced, especially for years of 2004, 2007, 2008, 2013 the different are almost overlap, which indicated that the affects to surrounding NDVI by Qinghai–Tibet Railway is 4 km in bilateral sides. This statistical results supported the rationality of the setting of the "core area" and "background buffer". The conclusion is also partially supported by similar studies based on MODIS

Table 2
Multiple linear stepwise regression in XGSP.

	Coefficient		Model		ANOVA		
	a	b	R^2	RMSE	F-statistic	Sig.	T test
Buffer2	0.980	0.008	0.994	0.00178	2777.305	0.000	52.700
Buffer3	1.041	−0.011	0.992	0.00203	2071.982	0.000	45.519
Buffer4	1.068	−0.020	0.983	0.00267	1187.820	0.000	34.465
Buffer5	1.053	−0.014	0.979	0.00336	744.863	0.000	27.292
Buffer6	1.087	−0.028	0.981	0.00315	845.434	0.000	29.076
Buffer7	1.114	−0.033	0.975	0.00365	626.658	0.000	25.033
Buffer8	1.072	−0.018	0.970	0.00403	512.522	0.000	22.639

Number of observations: 18, Error degrees of freedom: 16.
RMSE: Root Mean Squared Error.
R^2: R-squared; Adjusted R-Squared: abbreviation.

Table 3
Multiple linear stepwise regression in GSPL.

	Coefficient		Model		ANOVA		
	a	b	R^2	RMSE	F-statistic	Sig.	T test
Buffer2	0.980	0.002	0.978	0.00243	725.923	0.000	26.943
Buffer3	0.977	−0.002	0.964	0.00321	429.329	0.000	20.730
Buffer4	1.011	−0.019	0.926	0.00451	210.040	0.000	14.493
Buffer5	1.006	−0.017	0.950	0.00479	303.665	0.000	17.426
Buffer6	1.031	−0.026	0.899	0.00539	142.098	0.000	17.426
Buffer7	1.007	−0.015	0.876	0.00596	113.429	0.000	10.650
Buffer8	1.008	−0.015	0.857	0.00640	96.179	0.000	9.807

Number of observations: 18, Error degrees of freedom: 16.
RMSE: Root Mean Squared Error.
R^2: R-squared; Adjusted R-Squared: abbreviation.

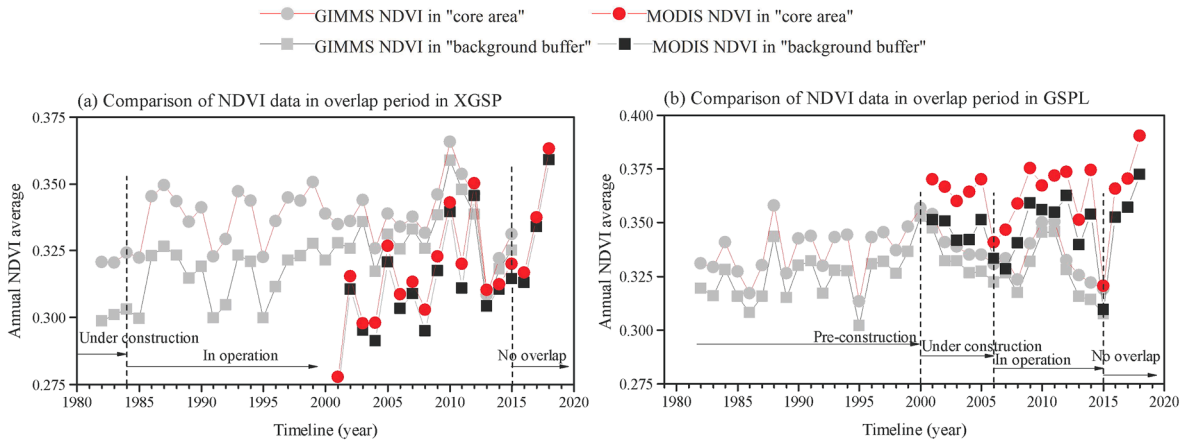

Fig. 14. Comparative analysis of GIMMS ANDVI and MODIS ANDVI in overlap period.

and Landsat data (Ding, et al., 2006; Li, et al., 2017).

2) multiple linear stepwise regression

Through the above analysis, it can be realized that due to the spatial closely adjacent, the linear correlation between the various radiuses of buffer NDVI is extremely high, and the mutation points are difficult to find. Therefore, we introduce the idea of multiple linear stepwise regression, with MODIS NDVI (2001–2018) in the core area as the dependent variable and MODIS NDVI in the buffer as the independent variable, through stepwise regression, and gradually eliminate the small contribution and confidence Low-level independent variables. The regression analysis report is shown in Tables. 2 and 3 respectively.

The results of multiple linear stepwise regression confirmed the results of the related analysis of Scatter matrix. In the Buffer5, including R^2, RMSE, F-statistic and T test, a variety of indicators showed a sharp change. Therefore, setting a double-sided 4 km buffer zone on the Qinghai-Tibet Railway should be the optimal strategy.

3) Evaluated with MODIS dataset

On the basis of previous research results, an 8 km "core area" consistent with GIMMS NDVI was set along the Qinghai–Tibet Railway, and another "8–16 km" "background buffer" was obtained by extending outward with a radius of 8 km. For this purpose, MODIS and GIMMS overlapped NDVI datasets of 15a are obtained (Fig. 14).

MODIS ANDVI and GIMMS ANDVI have an overlap period of 15 years (2001–2015), so that we can proofread the research results of single source product data. It can be seen from Fig. 14 that the trends of the two different source data are consistent, that is, the ANDVI in "core area" is lower than "background buffer". Under construction, the ANDVI shown a downward trend, while in operation the ANDVI shown an upward trend (of which 2010–2014, affected by the decrease in temperature fluctuations and the continuous decline in precipitation, the ANDVI has dropped significantly over time).

The regression equations between the two source product data can

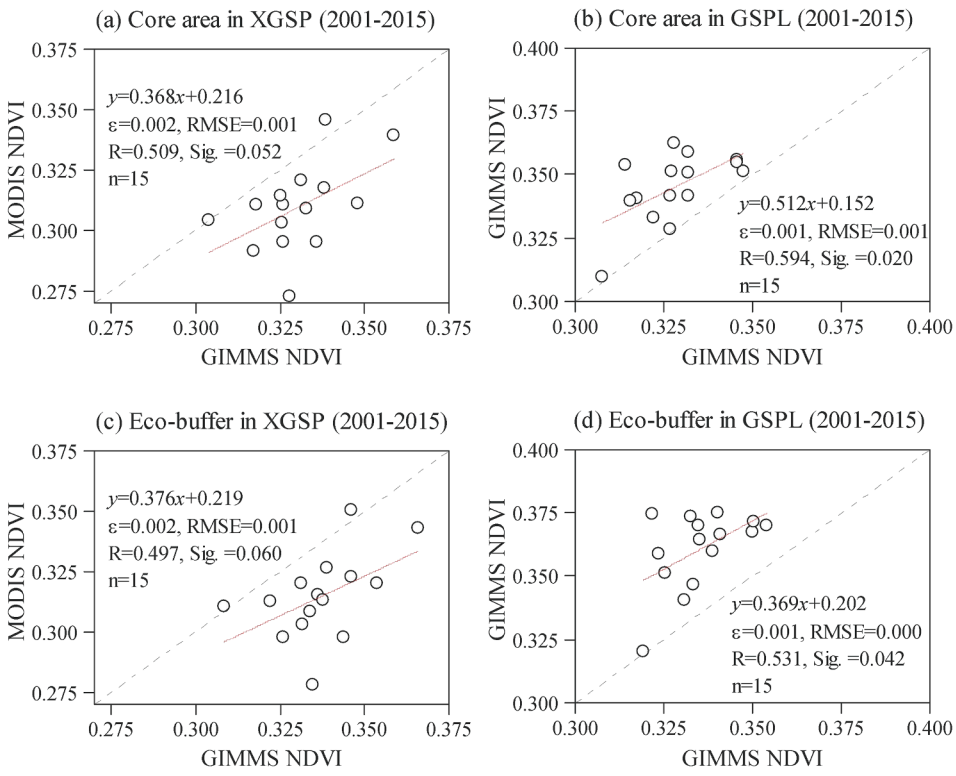

Fig. 15. Regression analysis of GIMMS ANDVI and MODIS ANDVI in overlap period.

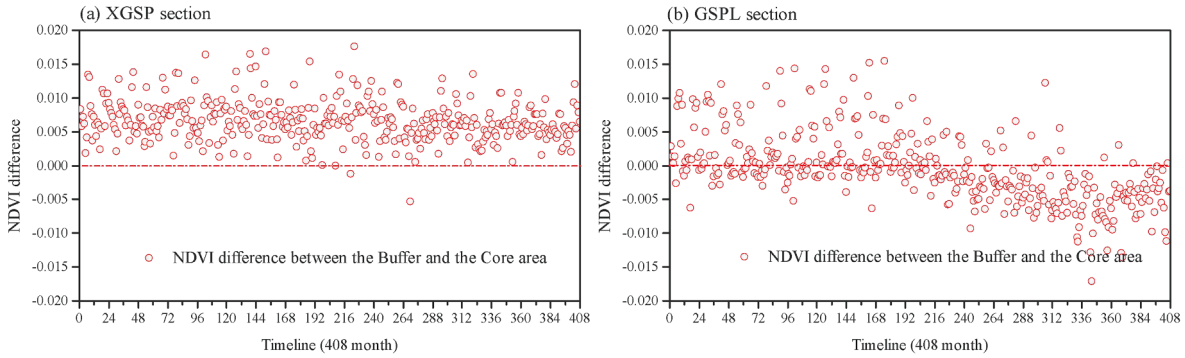

Fig. 16 The NDVI spatial heterogeneity between "core area" and "background buffer"

Fig. 16. The NDVI spatial heterogeneity between “core area” and “background buffer”

be described as follows: the coefficient of determination between “core area” and the eco-buffer (i.e. the ecological check area, CK)[10] is R = 0.509 (significant level Sig. = 0.052, n = 15) and R = 0.497 (Sig. = 0.060, n = 15) in the XGSP; the coefficient of determination between “core area” and the eco-buffer is R = 0.594 (Sig. = 0.020, n = 15) and R = 0.531 (Sig. = 0.042, n = 15) in the GSPL (see Fig. 15). It is worth noting that in the three years after 2015, MODIS NDVI has experienced a dramatic increase across the Qinghai–Tibet Railway.

5.2. Spatial heterogeneity of NDVI

The “core area” of the Qinghai–Tibet Railway is an 8 km belt shape area, and the “background buffer” is an 8 km wide ring area on both sides. The total width of the two areas is 24 km. The 8 km “core area” fully covers the area affected by the construction and operation of the Qinghai–Tibet Railway. The 8 to 16 km “background buffer” is far from the influence of railway construction and operation, but the climatic conditions are similar. Therefore, the “background buffer” can be deemed to the CK affected by climate.

Due to the large span of the study area, although the vegetation on the Qinghai–Tibet Plateau belongs to a large-area zonal distribution, the surface still has spatial heterogeneity (the difference caused by the spatial heterogeneity may not be considered for the max–min value method, but for the average method, and accumulate value method, which cannot be ignored). We found the spatial heterogeneity exists by calculating monthly difference of “core area” and “background buffer” of XGSP and GSPL (Fig. 16).

It can be seen from Fig. 16 that in XGSP, NDVI in most of month is dominated by positive values. NDVI of the “core area” is always greater than that of the “background buffer” and only shown a narrowing gap in the trend during 34a. In GSPL the difference is positive in domination for

[10] The ecological check area, CK

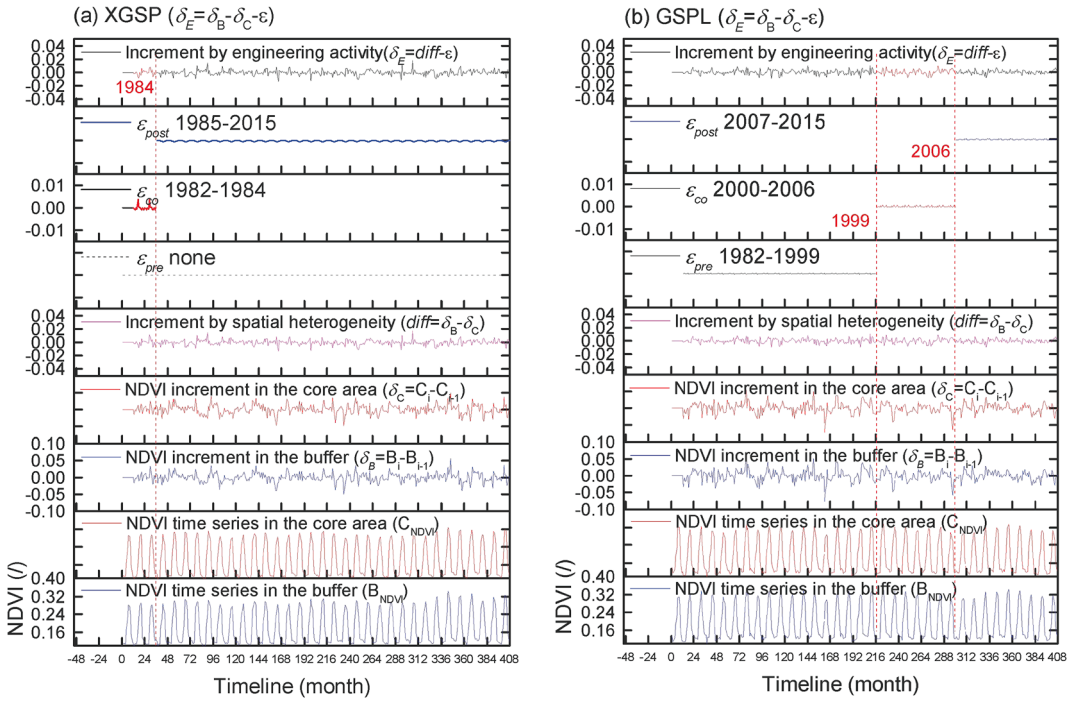

(a) Component of the 'Engineering Activities' in XGSP (a) Component of the 'Engineering Activities' in GSPL

Fig. 17. Extracting the component of the 'Engineering Activities' in NDVI.

early stage, and NDVI of "core area" is greater than that of "background buffer". While for the middle and late periods (2000 is the time inflection point), the difference is negative values in domination, NDVI of "core area" is smaller than that of "background buffer". Due to similar climatic conditions, climate variables are offset, the difference of NDVI between "core area" and "background buffer" needs to be treated separately: pre-construction, the difference is mainly due to the spatial heterogeneity of vegetation; under construction and in operation, the difference includes both spatial heterogeneity of vegetation and the impact of engineering activities.

5.3. Impact of engineering activities

For the contribution of natural change and human activity to time series NDVI, some studies have adopted the method of regression analysis to remove climatic factor, and attributed the residual as human activity factor (Liu et al., 2016; Yi et al., 2014). A common drawback of this method is that in areas where there is no human activity, contribution of human activity would still have preserved for residual not equal to zero. Therefore, in this research, an innovative temporal-spatial invariant approach is used to distinguish the contribution of natural and anthropogenic factors. The process progress of this method can be described as follows:

(1) The inter-annual NDVI is cyclical, if the perennial vegetation biomass is assumed to $NDVI_{mass}$, and the effect of superimposed climate change is $NDVI_{\text{climate}}$ during the same time. Since the influencing factors of "background buffer" and "core area" are different, for "background buffer", time series NDVI is B_{NDVI}, which is not affected by engineering activities, so there $B_{NDVI} = NDVI_{mass} + NDVI_{climate}$; while for "core area" where is no impact of engineering activities pre-construction, time series NDVI is C_{NDVI}. Under construction and in operation, $NDVI_{engineering}$ is affected by engineering activities, so $C_{NDVI} = NDVI_{mass} + NDVI_{\text{climate}} + NDVI_{engineering}$.

(2) Due to the similarity of short-term climatic conditions, we subtract the $NDVI_{(i-1)}$ of the previous year from the current year $NDVI_{(i)}$ to eliminate most of the impacts of climate change, and obtain the comprehensive increments NDVI of "background buffer" δ_B and "core area" δ_C for current year. The comprehensive increments NDVI was considered as Biomass accumulated of current year. So for "background buffer", $\delta_B = B_i - B_{i-1}$ (i = 1983, 1984, …, 2015), and for "core area", $\delta_C = C_i - C_{i-1}$ (i = 1983, 1984, …, 2015).

(3) It is different for the "background buffer" and the "core area". By subtracting the increment of the "core area" from the annual NDVI integrated increment of "background buffer", the cumulative impact of biomass can be eliminated, leaving only the increment of spatial heterogeneity of vegetation. While this is different for "background buffer" and "core area", for "background buffer", only the NDVI incremental diff caused by spatial heterogeneity of vegetation is: $diff = \delta_B - \delta_C$; while for "core area", the NDVI increment (a residual of a 12-month cycle) of vegetation is spatial heterogeneity in the pre-construction, but when the engineering activity increment is introduced during the under-construction and in-operation, the *diff* during the under-construction and in-operation should include the increment of engineering activities and the increment of spatial heterogeneity of vegetation.

(4) The contribution of spatial heterogeneity increment of the vegetation was same for each year, hence, we calculated the cyclic average residuals of n years pre-construction (a one-dimension vector composed of 12 elements), subtracted the *diff* during co-construction (i.e. under-construction) and post-construction (i.e., in-operation), and obtained the incremental engineering activity as $\delta_E = diff - \varepsilon$. Where, $\varepsilon = (\overline{\varepsilon_1}, \overline{\varepsilon_1}, \overline{\varepsilon_2}, ..., \overline{\varepsilon_{12}})$, $\overline{\varepsilon_i} = \pm\sqrt{\frac{\sum_{i=1}^{n}(x_i - \overline{x})^2}{n-1}}$, n is number of construction years, for instance, the 19 years from 1982 to 2000 were pre-construction in GSPL and ε was the average of these 19 years. In order to treat differently, we express the residuals before, during and after construction as ε_{pre}, ε_{co}, ε_{post}.

The extracted influence factor of engineering activities of the XGSP and GSPL of Qinghai–Tibet Railway are shown as Fig. 17.

Quantitative results shown that: (1) The total NDVI of the XGSP is 72.829 for "background buffer" and 72.575 for "core area", the net increment is 14% and 23% respectively among 34 years; the impact of climate is –9.3% and the impact of engineering activities is –0.24% in

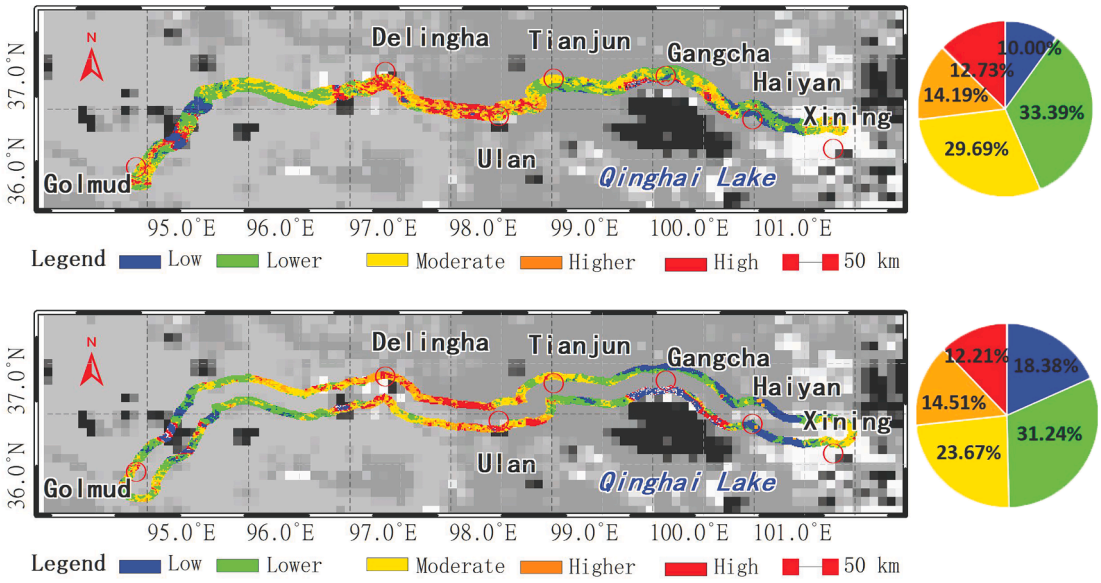

Fig. 18. MODIS NDVI coefficient of variation in XGSP during 18-year.

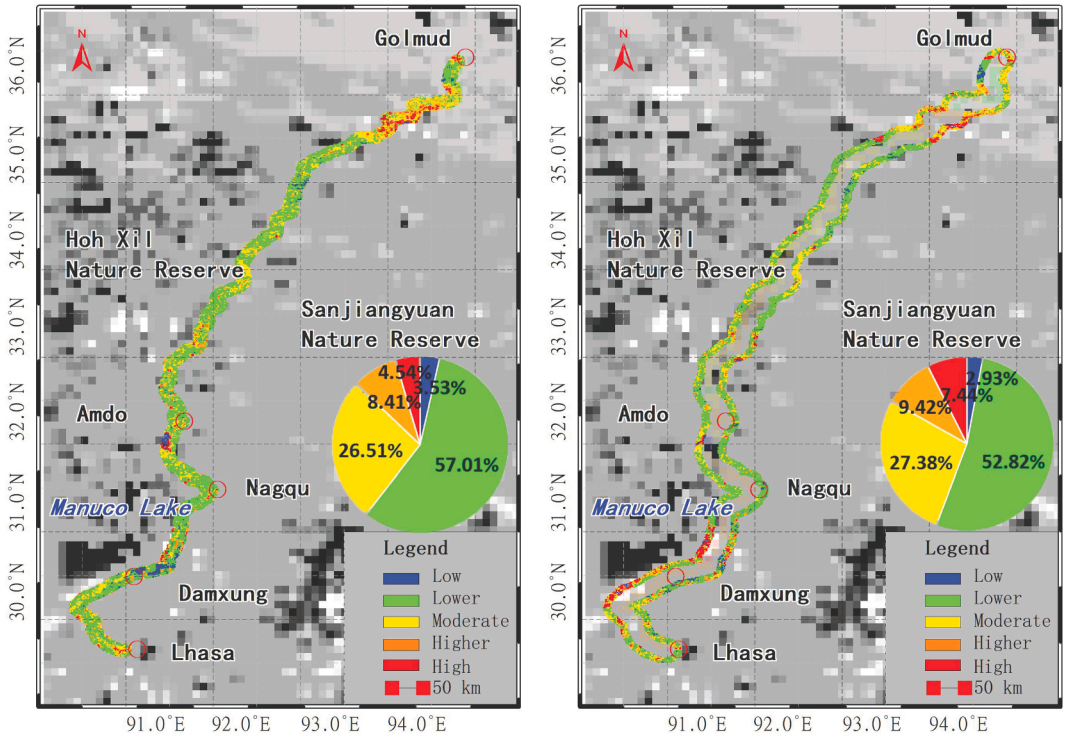

Fig. 19. MODIS NDVI coefficient of variation in GSPL during 18-year.

"core area". (2) The total NDVI of the GSPL is 78.566 and 76.047, and the net increment is –3.56% and –2.33% for "background buffer" and "core area" respectively during 34 years; the climate impact is –1.19%, and the impact of engineering activities is –0.04% of the "core area".

5.4. Variation coefficient of MODIS NDVI

The NDVI variation coefficients C_v (2001–2018) of "core area" and "background buffer" of the two sections calculated with MODIS dataset are shown in Figs. 18 and 19 (the background is 1:1 million GLC30[11]).

Based on the same grading criteria (Ana et al., 2017), the XGSP is dominated by lower to moderate fluctuations (mainly located near Qaidam Basin and Qinghai Lake) is more than 70%, and higher to high fluctuations (mainly distributed along Delingha to Tianjun) is about 26%; the GSPL is dominated by lower fluctuations (alone Amdo-Lhasa segment) and moderate fluctuations (mainly distributed in the Hoh Xil

[11] GlobeLand30 refers to the land cover of the earth between latitude 80N to 80S. http://www.globallandcover.com/GLC30Download/index.aspx

nature reserve and Sanjiangyuan nature reserve) is about 80% and higher to high fluctuations are mainly distributed along Manuco lake and intersection with Kunlun Mountains). On the whole, the volatility of "core area" is slightly higher than "background buffer" in the XGSP; and the volatility of "background buffer" is slightly higher than "core area" in the GSPL (see S5).

Comparing the coefficients of variation of GIMMS NDVI and MODIS NDVI, the following conclusions can be drawn: Whether it is in XGSP or GSPL, the C_v fluctuation degree in the core area is greater than that in the buffer; C_v (1982–2015) is dominated by higher fluctuations; and C_v (2001–2018) is dominated by low to lower fluctuations (see S6).

6. Conclusions

(1) In general, the annual average NDVI of the XGSP of the Qinghai–Tibet Railway shown a slowly increase trend. Studies demonstrated that after the operation of the XGSP of the Qinghai–Tibet Railway, the vegetation growth condition was recovery, and the vegetation has an improvement trend. The annual NDVI of the GSPL of the Qinghai–Tibet Railway shown an overall downward trend. A piecewise linear fitting analysis results indicated that there is a correlation between NDVI and railway construction. Railway construction has a significant impact on the growth of vegetation. That is, the growth of the vegetation is good before railway construction, while vegetation growth has a downward trend during the construction engineering activity, and the vegetation has a tendency to recover after the construction.

(2) The climate along the Qinghai–Tibet Railway is developing toward warming and humidification, and the annual average temperature and precipitation are both increasing. Correlation analysis between NDVI and climate indicated that the growth of vegetation in the core area of the XGSP is more affected by temperature (T) than precipitation (P) ($r_{NDVI/T} = 0.651$, $P < 0.01$; $r_{NDVI/P} = 0.395$, $P < 0.05$), the growth of vegetation in the buffer zone of the XGSP is affected by the combined effect of temperature and precipitation ($r_{NDVI/T} = 0.336$, $P < 0.05$; $r_{NDVI/P} = 0.344$, $P < 0.05$); while the growth of the vegetation in GSPL is not related to the average annual temperature and precipitation.

(3) Results of NDVI variation coefficient analysis along the Qinghai–Tibet Railway demonstrated that the XGSP is significantly affected by climate change. The high fluctuations and relatively high fluctuations in the "core area" is 77.08%, and high fluctuations and relatively high fluctuations in the "background buffer" is 72.5%. In the GSPL, the high-volatility changes and relatively high fluctuations in the "core area" and "background buffer" is 93.39% and 91.2%, respectively. The "background buffer" is mainly affected by climate change, and the "core area" is combined affected by climate change and engineering activities.

(4) Impact of engineering activities was obtained. In spatial dimension, the "background buffer" was used as the CK of the "core area", and in temporal dimension, the pre-construction NDVI was settled as background value of ecological increment during the under-construction and in-operation to remove the effect of spatial heterogeneity of vegetation coverage, impact of climate change and effects of periodic cumulative. The results demonstrated that the climatic impact of the "core area" of the XGSP is –9.3%, and the impact of engineering activities is –0.24%; the climatic impact of the "core area" of the GSPL is –1.19%, and the impact of engineering activities is –0.04%. In summary, NDVI3g + responds to climate change and engineering activities along the Qinghai–Tibet Railway, with climate change in domination and engineering activities as supplement.

The GIMMS NDVI3g + data used for NDVI Change research along the Qinghai–Tibet Railway with a long time series but low spatial resolution, making it impossible to analyze the growth of detailed vegetation types. Results obtained on the basis of inter-annual, inner-annual maximum and average NDVI has limitation of effective evaluation for long time, large spatial span, and lack of field measurement Future investigation is intended to introduce data with higher spatial resolution (such as SPOT NDVI, Landsat NDVI) to refine the research results.

Funding

This work was supported by National Natural Science Foundation of China [Grant Number 41601450, 41975036]; Cooperative Exchange Program between the National Natural Science Foundation of China and the Royal Society of UK [Grant Number 42011530174]; the Key Technology R and D Program of Henan Province [Grant Number 182102310860]; Innovative research team of Henan Polytechnic University, [Grant Number T2018-4] and China Scholarship Council Grant [Grant Number 201808410212].

CRediT authorship contribution statement

Chao Ma: Conceptualization, Methodology, Writing - original draft. **Tingting Li:** Investigation, Validation, Visualization, Writing - original draft. **Pei Liu:** Data curation, Funding acquisition, Software, Writing - review & editing.

Declaration of Competing Interest

The authors declare that they have no known competing financial interests or personal relationships that could have appeared to influence the work reported in this paper.

Acknowledgements

The authors would like to thank the anonymous reviewers and editor for constructive comments and suggestions.

Appendix A. Supplementary data

Supplementary data to this article can be found online at https://doi.org/10.1016/j.ecolind.2021.107821.

References

Ana, M., Maria, U., Unai, P.G., 2017. Stochastic spatio-temporal models for analysing NDVI distribution of GIMMS NDVI3g images. Remote Sensing 9, 76. https://doi.org/10.3390/rs9010076.

Chen, F., Lin, H., Li, Z., Chen, Q., Zhou, J., 2012. Interaction between permafrost and infrastructure along the Qinghai-Tibet Railway detected via jointly analysis of C- and L-band small baseline SAR interferometry. Remote Sens. Environ. 123, 532–540. https://doi.org/10.1016/j.rse.2012.04.020.

Chen, H., Li, S., Zheng, D., 2003. Features of ecosystems alongside qinghai-xizang highway and railway and the impacts of road construction on them. J. Mountain Sci. 21 (5), 559–567. https://doi.org/10.16089/j.cnki.1008-2786.2003.05.007.

Dardel, C., Kergoat, L., Hiernaux, P., Mougin, E., Grippa, M., Tucker, C.J., 2014. Re-greening Sahel: 30years of remote sensing data and field observations (Mali, Niger). Remote Sens. Environ. 140, 350–364. https://doi.org/10.1016/j.rse.2013.09.011.

Ding, M., Zhang, Y., Shen, Z., Liu, L., Zhang, W., Wang, Z., Bai, W., Zheng, D., 2006. Land cover change along the Qinghai-Tibet Highway and Railway from 1981 to 2001. J. Geograph. Sci. 16, 387–395. https://doi.org/10.1007/s11442-006-0401-y.

Ding, M.J., Shen, Z.X., Zhang, Y.L., Liu, L.S., Zhang, W., Wang, Z.F., Bai, W.Q., 2005. Vegetation Change along the Qinghai-Xizang Highway and Railway from 1981 to 2001. Resourc. Sci. 27, 128–133. https://doi.org/10.1360/biodiv.050058.

Goetz, S.J., Fiske, G.J., Bunn, A.G., 2006. Using satellite time-series data sets to analyze fire disturbance and forest recovery across Canada. Remote Sens. Environ. 101, 352–365. https://doi.org/10.1016/j.rse.2006.01.011.

Hou, X., Li, M., Gao, M., Yu, L., Bi, X., 2013. Spatial-temporal dynamics of NDVI and Chl-a concentration from 1998 to 2009 in the East coastal zone of China: integrating terrestrial and oceanic components. Environ. Monit. Assess. 185, 267–277. https://doi.org/10.1007/s10661-012-2551-y.

Kobayashi, H., Dye, D.G., 2005. Atmospheric conditions for monitoring the long-term vegetation dynamics in the Amazon using normalized difference vegetation index. Remote Sens. Environ. 97, 519–525. https://doi.org/10.1016/j.rse.2005.06.007.

Lei, Y., Zhu, Y., Wang, B., Yao, T., Yang, K., Zhang, X., Zhai, J., Ma, N., 2019. Extreme lake level changes on the Tibetan plateau associated with the 2015/2016 El Niño. Geophys. Res. Lett. 46 https://doi.org/10.1029/2019GL081946.

Li, M., Sheng, Y., 2008. Study on application of gaussian fitting algorithm to building model of spectral analysis. Spectrosc. Spectral Anal. 28, 146–149. https://doi.org/10.3964/j.issn.1000-0593(2008)10-2352-04.

Li, S., Wang, C., Xu, X., Shi, L., Yin, N., 2019. Experimental and statistical studies on the thermal properties of frozen clay in Qinghai-Tibet Plateau. Appl. Clay Sci. 177, 1–11. https://doi.org/10.1016/j.clay.2019.05.002.

Li, Y., Zhou, J., Wu, X., 2017. Effects of the construction of Qinghai-Tibet railway on the vegetation ecosystem and eco-resilience. Geograph. Res. 46, 5889–5898. https://doi.org/10.11821/dlyj201711008.

Liu, X., Ren, Z., Lin, Z., Liu, Y., Zhang, D., 2013. The spatial-temporal changes of vegetation coverage in the Three-River Headwater Region in recent 12 years (2000–2011). J. Geog. Sci. 68, 897–908.

Liu, Y., Li, C., Liu, Z., Deng, X., 2016. Assessment of spatio-temporal variations in vegetation cover in Xinjiang from 1982 to 2013 based on GIMMS-NDVI. Acta Ecol. Sin. 36, 6198–6208. https://doi.org/10.5846/stxb201506071149.

Luo, J., Niu, F., Liu, M., Lin, Z., Yin, G., 2018a. Field experimental study on long-term cooling and deformation characteristics of crushed-rock revetment embankment at the Qinghai-Tibet Railway. Appl. Therm. Eng. 139, 256–263. https://doi.org/10.1016/j.applthermaleng.2018.04.138.

Luo, L., Ma, W., Zhuang, Y., Zhang, Y., Yi, S., Xu, J., Long, Y., Ma, D., Zhang, Z., 2018b. The impacts of climate change and human activities on alpine vegetation and permafrost in the Qinghai-Tibet Engineering Corridor. Ecol. Ind. 93, 24–35. https://doi.org/10.1016/j.ecolind.2018.04.067.

Lv, Y., Dong, G., Yang, S., Zhou, Q., Cai, M., 2014. Spatio-temporal variation in NDVI in the Yarlung Zangbo River basin and its relationship with precipitation and elevation. Resourc. Sci. 36, 179–187.

Niu, F., Gao, Z., Lin, Z., Luo, J., Fan, X., 2019. Vegetation influence on the soil hydrological regime in permafrost regions of the Qinghai-Tibet Plateau, China. Geoderma 354, 113892. https://doi.org/10.1016/j.geoderma.2019.113892.

Piao, S., Fang, J., 2002. Terrestrial net primary production and its spatio-temporal patterns in Qinghai-Xizang Plateau, China during 1982–1999. Nat. Resourc. 17, 373–380. https://doi.org/10.3321/j.issn:1000-3037.2002.03.020.

Qin, Y., Zheng, B., 2010. The Qinghai-Tibet Railway: a landmark project and its subsequent environmental challenges. Environ. Dev. Sustain. 12, 859–873. https://doi.org/10.1007/s10668-009-9228-x.

Sun, B., Yang, L., Liu, Q., Xu, X., 2010. Numerical modelling for crushed rock layer thickness of highway embankments in permafrost regions of the Qinghai-Tibet Plateau. Eng. Geol. 114, 181–190. https://doi.org/10.1016/j.enggeo.2010.04.014.

Tucker, C.J., Pinzon, J.E., Brown, M.E., Slayback, D.A., Pak, E.W., Mahoney, R., Vermote, E.F., El Saleous, N., 2005. An extended AVHRR 8-km NDVI dataset compatible with MODIS and SPOT vegetation NDVI data. Int. J. Remote Sens. 26, 4485–4498. https://doi.org/10.1080/01431160500168686.

Tucker, C.J., Slayback, D.A., Pinzon, J.E., Los, S.O., Myneni, R.B., Taylor, M.G., 2001. Higher northern latitude normalized difference vegetation index and growing season trends from 1982 to 1999. Int. J. Biometeorol. 45, 184–190. https://doi.org/10.1007/s00484-001-0109-8.

Tibet Autonomous Region Railway Construction and Operation Leading Group Office Tibet Autonomous Region Development and Reform Commission, 2016. Qinghai-Tibet railway operation ten years to boost Tibet's economic and social development report. China Railway 5, 8–11.

Wang, G., Gillespie, A.R., Liang, S., Mushkin, A., Wu, Q., 2015. Effect of the Qinghai-Tibet Railway on vegetation abundance. Int. J. Remote Sens. 36, 5222–5238. https://doi.org/10.1080/01431161.2015.1041179.

Wang, L., Wu, Z., Sun, J., Liu, X., Wang, Z., 2009. Characteristics of ground motion at permafrost sites along the Qinghai-Tibet railway. Soil Dyn. Earthq. Eng. 29, 974–981. https://doi.org/10.1016/j.soildyn.2008.11.009.

Wang, W., Wu, T., Chen, Y., Li, R., Xie, C., Qiao, Y., Zhu, X., Hao, J., Ni, J., 2019. Spatial variations and controlling factors of ground ice isotopes in permafrost areas of the central Qinghai-Tibet Plateau. Sci. Total Environ. 688, 542–554. https://doi.org/10.1016/j.scitotenv.2019.06.196.

Wu, J., Duan, D., Lu, J., Luo, Y., Wen, X., Guo, X., Boman, B.J., 2016. Inorganic pollution around the Qinghai-Tibet Plateau: an overview of the current observations. Sci. Total Environ. 550, 628–636. https://doi.org/10.1016/j.scitotenv.2016.01.136.

Wu, Q., Liu, Y., Hu, Z., 2011. The thermal effect of differential solar exposure on embankments along the Qinghai-Tibet Railway. Cold Reg. Sci. Technol. 66, 30–38. https://doi.org/10.1016/j.coldregions.2011.01.001.

Wu, Q., Zhang, T., Liu, Y., 2010. Permafrost temperatures and thickness on the Qinghai-Tibet Plateau. Global Planet. Change 72, 32–38. https://doi.org/10.1016/j.gloplacha.2010.03.001.

Yan, H., Liu, J., Cao, M., 2005. Remotely sensed multiple cropping index variations in China during 1981–2000. Acta Geograph. Sin. 60, 559–566. https://doi.org/10.3321/j.issn:0375-5444.2005.04.004.2015.

Güçlü, Y.S., 2020. Improved visualization for trend analysis by comparing with classical Mann-Kendall test and ITA. J. Hydrol. 584, 124674 https://doi.org/10.1016/j.jhydrol.2020.124674.

Yi, L., Ren, Z., Zhang, C., Liu, W., 2014. Vegetation cover, climate and human activities on the Loess Plateau. Resourc. Sci. 36, 166–174.

Zhang, Y., Yan, J., Liu, Y., Zheng, D., 2002c. Impact of Qinghai Tibet Railway on regional land use and landscape pattern – Taking Xining Golmud section as an example, China's accession to WTO and China's science and technology and sustainable development - challenges and opportunities, responsibilities and Countermeasures (Volume I). Chengdu, Sichuan, China.

Zhang, G.L., Zhang, Y.J., Dong, J.W., Xiao, X.M., 2013a. Green-up dates in the Tibetan Plateau have continuously advanced from 1982 to 2011. PNAS 110 (11), 4309–4314. https://doi.org/10.1073/pnas.1210423110.

Zhang, H., Wang, Z., Zhang, Y., Hu, Z., 2012a. The effects of the Qinghai-Tibet railway on heavy metals enrichment in soils. Sci. Total Environ. 439, 240–248. https://doi.org/10.1016/j.scitotenv.2012.09.027.

Zhang, K., Qu, J., Han, Q., An, Z., 2012b. Wind energy environments and aeolian sand characteristics along the Qinghai-Tibet Railway, China. Sed. Geol. 273–274, 91–96. https://doi.org/10.1016/j.sedgeo.2012.07.003.

Zhang, M., Wang, J., Lai, Y., 2019. Hydro-thermal boundary conditions at different underlying surfaces in a permafrost region of the Qinghai-Tibet Plateau. Sci. Total Environ. 670, 1190–1203. https://doi.org/10.1016/j.scitotenv.2019.03.090.

Zhang, Y., 2002. Negative impact of Qinghai- Tibetan Railway construction on ecological environment of Qinghai-Tibetan Plateau. Bull. Soil Water Conserv. 22, 50–53. https://doi.org/10.3969/j.issn.1000-288X.2002.04.013.

Zhang, Y., Gao, J., Liu, L., Wang, Z., Ding, M., Yang, X., 2013b. NDVI-based vegetation changes and their responses to climate change from 1982 to 2011: a case study in the Koshi River Basin in the middle Himalayas. Glob. Planet. Change 108, 139–148. https://doi.org/10.1016/j.gloplacha.2013.06.012.

Zhang, Y., Yan, J., Liu, L., Bai, W., Li, S., Zheng, D., 2002. Impact of Qinghai-Xizang Highway on land use and landscape pattern change:from Golmud to Tanggulashan Pass. Acta Geograph. Sin. 57, 253–266. https://doi.org/10.3321/j.issn:0375-5444.2002.03.001.